Applied Mathematics and Computation 457 (2023) 128207

Contents lists available at ScienceDirect

Applied Mathematics and Computation

journal homepage: www.elsevier.com/locate/amc

Structural schemes for one dimension stationary equations

Stéphane Clain [a,*], Rui M.S. Pereira [b,d], Paulo A. Pereira [c,d], Diogo Lopes [e]

[a] CMUC –Mathematical centre, Coimbra University, Apartado 3008 EC Santa Cruz, Coimbra 3001-501, Portugal
[b] CFUM-UP – Physics Centre, Minho and Porto Universities, Azurém Campus, University of Minho, Guimarães 4800-058, Portugal
[c] CMAT – Mathematics centre, Minho University, Azurém Campus, Guimarães 4800-058, Portugal
[d] DMAT – Mathematics department, Minho University, Azurém Campus, Guimarães 4800-058, Portugal
[e] 2AI – Applied Artificial Intelligence Laboratory, Instituto Politécnico do Cávado e do Ave, Barcelos 4750-810, Portugal

ARTICLE INFO

Article history:
Received 2 January 2023
Revised 21 June 2023
Accepted 22 June 2023

Keywords:
Structural equation
Compact scheme
Very high-order
Finite difference

ABSTRACT

In this paper, we propose a new paradigm for finite differences numerical methods, based on compact schemes to provide high order accurate approximations of a smooth solution. The method involves its derivatives approximations at the grid points and the construction of structural equations deriving from the kernels of a matrix that gathers the variables belonging to a small stencil. Numerical schemes involve combinations of physical equations and the structural relations. We have analysed the spectral resolution of the most common structural equations and performed numerical tests to address both the stability and accuracy issues for popular linear and non-linear problems. Several benchmarks are presented that ensure that the developed technology can cope with several problems that may involve non-linearity.

1. Introduction

The present study is dedicated to the design of a new class of compact finite difference methods. Following Y. Adam [55], S. G. Rubin and R. A. Graves [45] and R. Hirsh [25], we seek for the approximations $Z_i \approx \varphi(x_i)$ of a steady-state problem (convection diffusion reaction for instance) by introducing new unknowns D_i and S_i of the first- and second-derivative approximations at point x_i respectively. Additional equations involving implicit relation between Z, D and S lead to a more compact stencil regarding the stencil we should use to provide the same accuracy. In the original design, Adam considers two, fourth-order, independent relations with a three point stencil: the first one connects the function and the first derivative while the second one links the function with the second derivative.

In [7,9], Chu and Fan propose a new three-point sixth-order Combined Compact Scheme (CCS) that involves at the same time the function and all the derivatives (first and second derivatives) as

$$\sum_{\ell=-s}^{r} \alpha_{i+\ell} Z_{i+\ell} + \sum_{\ell=-s}^{r} \beta_{i+\ell} D_{i+\ell} + \sum_{\ell=-s}^{r} \gamma_{i+\ell} S_{i+\ell} = 0. \tag{1}$$

* Corresponding author.
E-mail addresses: clain@mat.uc.pt (S. Clain), rmp@math.uminho.pt (R.M.S. Pereira), ppereira@math.uminho.pt (P.A. Pereira), dlopes@ipca.pt (D. Lopes).

https://doi.org/10.1016/j.amc.2023.128207

By that way, the locality of the information improves the spectral resolution. The authors then derive two relations from (1). They combine them with the physical one and deliver a sixth-order compact scheme (see also [5]). The extension of (CCS) from uniform grid to a non-uniform grid scheme has been tackled by different authors [9,19]. In general, they use a mapping from a non-uniform grid to a uniform one in order to apply the compact schemes for uniform grids [18,49,59]. Another variant is the development of staggered compact schemes for incompressible flow to enforce the stability of the pressure [4,28,31,37,48].

No significative improvements of the compact scheme technology have been done in the two last decades, where investigation studies mainly concerned the applications (see the historical notes in appendix). The *modus operandi* is almost the same as the one proposed by Lele [29] or Chu and Fan [7] involving an *a priori* linear combination of the function and its derivatives' approximations where one has to determine the coefficients using the Taylor expansion or some additional criteria to improve the spectral resolution.

In this study, we propose a new paradigm to develop compact schemes with a different approach compared to the traditional techniques. In some way, we propose an extension of the High Order Compact (HOC) scheme method with a generic procedure to compute the coefficients.

1. We definitely separate the relations deriving from the physics of the problem —tagged as Physical Equations PE, from the relations between the function and the derivatives for any given stencil —tagged as Structural Equations SE. The expression "structural" is motivated by the fact that the relations are independent of the nature of the problem and only rely on the structure of the grid. In other words, such relations are determined once for all, given the grid and the stencils.
2. We derive the structural relations from the successive kernels of a matrix, where no analytic expression is required. The relations are derived from the determination of the eigenvectors of the null space, and the algorithm is performed for any type of grid. Therefore, the coefficients are not given explicitly in function of the grid nodes, but are computed by a pre-processing routine.
3. We produce an ordered set of structural equations where the first one enjoys the highest accuracy (let's say m), whereas the k-th structural equation is of order $m+1-k$.
4. The structural equations involve first- and second-order derivates (extension to any order of derivative are not considered in the present study) and can be easily designed in function of the problem type, *i.e.* the user chooses the stencil shape and the derivatives he wants to connect for his specific problem.
5. The discrete problem is composed of physical and structural equations that provide a global, very sparse, (non-)linear system one has to solve. Different constructions for the same problem are then enabled by varying the choice of the structural equations to prioritize some property (accuracy, robustness, spectral resolution, computational effort).

The paper is structured as follows. Section 2 presents the general framework to design the structural equations, while Section 3 is dedicated to the spectral resolution analysis. Section 4 concerns the construction of the schemes by combining physical equations (inner equations and boundary conditions) with the structural ones. Benchmarking is carried out in the 5-th section to assess the accuracy and stability of the method for a large set of examples. We draw some conclusions in the last section.

2. Structural and physical equations

To introduce the philosophy of the method, we consider, as an example, the simple linear problem $r\phi + u\phi' - \kappa\phi'' = f$ on domain $\Omega = [x_L, x_R]$ and let $x_i = i\Delta x$, $i = 0, \cdots, I$ be a subdivision of Ω with $\Delta x = (x_R - x_L)/I$. The simplest and well-known centred scheme is given by,

$$r\phi_i + u\frac{\phi_{i+1} - \phi_{i-1}}{2\Delta x} - \kappa\frac{\phi_{i+1} + \phi_{i-1} - 2\phi_i}{(\Delta x)^2} = f_i,$$

where ϕ_i stands for an approximation of $\phi(x_i)$. In fact, the scheme blends two very different ingredients. On the one hand, we introduce approximation for the function, the first- and second-derivative denoted by Z_i, D_i and S_i respectively, and state that such quantities substitute the exact solution in the equation. We obtain the discrete physical equation PE

$$rZ_i + uD_i - \kappa S_i = f_i. \tag{2}$$

On the other hand, we use explicit relations to approximate the derivatives by setting

$$D_i = \frac{Z_{i+1} - Z_{i-1}}{2\Delta x}, \tag{3}$$

$$S_i = \frac{Z_{i+1} + Z_{i-1} - 2Z_i}{(\Delta x)^2}. \tag{4}$$

Equation (2) mimics the physical equation at the discrete level. On the contrary, equations (3)-(4) are independent of the underlying physical problem but rely on the connections between the node i and the nodes in the vicinity. The relations depend on the structure of the grid and the relative position of the points.

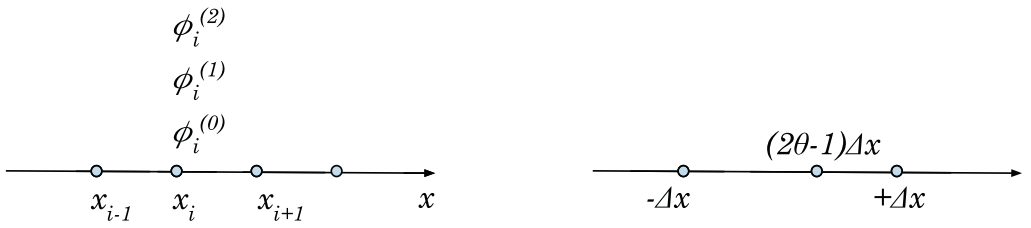

Fig. 1. Grid notations with the unknowns associated to node i (left panel). Localization of the intermediate node i regarding the extreme node at $-\Delta x$ and Δx. The intermediate point is characterized by parameter $\theta \in [0, 1]$(right panel).

From that point of view, we tag equation (2) as physical equation PE1 whereas, we tag equations (3)-(4) as structural equations SE1 and SE2. Each node i supports three information (Z_i, D_i, S_i), $i = 1, \cdots, I-1$ and the global system, together with boundary conditions, assimilated as a second physical equation PE2, couples physical and structural equations.

2.1. Hermitian and combined structural equations

This section is devoted to a general method to derive Structural Equations SE that provide additional equations together with the physical equation. In the previous example, the structural equations provide explicit expressions for the first- and second-derivative, but one may introduce implicit relations, and, by that way, increase the number of Degrees Of Freedom by introducing local linear combinations between the unknowns Z_j, D_j and S_j, $j = i-1, i, i+1$. For example, the so-called compact hermitian scheme [14,42,55] consists in substituting relations (3)-(4) with the Hermitian Structural Equations HSE1 and HSE2

$$0 = \frac{Z_{i-1} - Z_{i+1}}{\Delta x} + \frac{D_{i-1} + 4D_i + D_{i+1}}{3}, \tag{5}$$

$$0 = \frac{-Z_{i-1} + 2Z_i - Z_{i+1}}{(\Delta x)^2} + \frac{S_{i-1} + 10S_i + S_{i+1}}{12}. \tag{6}$$

Notice that the physical equation remains the same, but we manage to achieve a fourth-order scheme using additional unknowns in the structural equations while preserving the stencil. Of course, substitution is now impossible, and the three equations are fully coupled, leading to a $3 \times I$ system to solve (leaving apart the question of the boundary condition which we shall tackle in the sequel).

A more entangled scheme, involving all the derivatives, was proposed by [7,36] and the Combined Structural Equations CSE1 and CSE2 read

$$0 = -15\frac{Z_{i+1} - Z_{i-1}}{(\Delta x)^2} + \frac{7D_{i+1} + 16D_i + 7D_{i-1}}{\Delta x} - (S_{i+1} - S_{i-1}) = 0, \tag{7}$$

$$0 = 24\frac{Z_{i+1} - 2Z_i + Z_{i-1}}{\Delta x^2} - 9\frac{D_{i+1} - D_{i-1}}{\Delta x} + (S_{i+1} - 8S_i + S_{i-1}) = 0. \tag{8}$$

Using the same physical equations PE1 (inner) and PE2 (boundary), we achieve a sixth-order of accuracy.

2.2. Design of general structural equations

We propose a global approach to design structural equations that we present within the context of one-dimensional problems. We assume that the domain is meshed with points x_i and set $\Delta x_{i+1/2} = x_{i+1} - x_i$. We introduce the more general notations $\phi_i^{(s)} \approx \phi^{(s)}(x_i)$ to handle approximations of the function and its derivatives, as presented in Fig. 1, left panel.

In the present study, we restrict the construction for the three-points two-derivatives situation. Extension to a more general situation is possible, but out of the scope of the paper. On the one hand, we define the linear functional

$$E(\phi, i) = \sum_{r=-1,0,1} \sum_{s=0,1,2} a_{i,r}^{(s)} \phi^{(s)}(x_{i+r}) \tag{9}$$

where $a_{i,r}^{(s)}$ are the 9 real coefficients to be determined. First, we fix the pattern of the relation (9), where we may omit some coefficients to reduce the number of unknowns. For example, the first Hermitian equation requires that the second-derivative terms are omitted, while the CCS method uses the whole 9 parameters as unknowns. Then, the remaining coefficients are determined by prescribing that the relation is exact for polynomial functions up to a fixed degree. We expect, by this way, to obtain relations between the function and its derivatives that provide very accurate approximations.

To present the algorithm that provides the structural equations, we assume that all the 9 coefficients participate in the construction of the scheme (no omission parameters). Given a node $i = 1, \cdots, I-1$, we denote by $\phi_{k,i}(x) = (x - x_i)^{k-1}$, $k = 1, \cdots, 9$ the polynomial functions and one has

$$E(\phi_{k,i}, i) = \sum_{s=0,1,2} a_{i,-1}^{(s)} \frac{(k-1)!}{(k-1-s)!}(-\Delta x_{i-1/2})^{k-1-s} + \sum_{s=0,1,2} a_{i,0}^{(s)} \frac{(k-1)!}{(k-1-s)!}(0)^{k-1-s} + \sum_{s=0,1,2} a_{i,-1}^{(s)} \frac{(k-1)!}{(k-1-s)!}(\Delta x_{i+1/2})^{k-1-s}$$

with the convention $\dfrac{(k-1)!}{(k-1-s)!}(\Delta x)^{k-1-s} = 0$ if $k \leq s$ and $(0)^{k-1-s} = 1$ if $k = s+1$. We define a local indexation by setting $(r,s) \to j = j(r,s) = 3s + r + 2$ and gathering the entries $a_{i,k}^{(s)}$ in a local vector denoted $\mathtt{a}_i[:]$ with the convention,

$$\mathtt{a}_i[j] = a_{i,r}^{(s)}, \quad j = j(r,s).$$

For example, $\mathtt{a}_i[1] = a_{i,-1}^{(0)}$ while the last term is $\mathtt{a}_i[9] = a_{i,+1}^{(2)}$. In the same way, we define the matrix $\mathtt{M}_i$ associated to node i with the entries

$$\mathtt{M}_i[k,j] = \frac{(k-1)!}{(k-1-s)!}(x_{i+r} - x_i)^{k-1-s}, \text{ with } j = j(r,s).$$

Remark. We adopt the convention $\mathtt{a}[:3]$ to represent the first 3 entries of the vector $\mathtt{a}$ while $\mathtt{a}[:]$ is the whole vector. Similarly, $\mathtt{M}_i[:6,:]$ represents the first 6 rows of the matrix $\mathtt{M}_i$.

Since a vector $\mathtt{a}_i[:]$ has 9 components, for any $k = 1, \cdots, 9$, equation (13) can be written in the matrix form

$$E(\phi_{k,i}, i) = \sum_{j=1}^{9} \mathtt{M}_i[k,j]\mathtt{a}_i[j] = \mathtt{M}_i[k,:]\mathtt{a}_i[:]$$

where $\mathtt{M}_i[k,:]$ is the k-th row of the square matrix $\mathtt{M}_i$. The matrix $\mathtt{M}$ is of Vandermonde type and assuming $\Delta x_{i-1/2} > 0$, $\Delta x_{i+1/2} > 0$, the 9×9 matrix $\mathtt{M}_i$ is not singular. Consequently, if one imposes $E(\phi_{k,i}, i) = 0$ for $k = 1, \cdots, 9$, then the linear system reads $\mathtt{M}_i\mathtt{a}_i = 0$ and the solution is trivially $\mathtt{a}_i = 0$ in $\mathbb{R}^9$.

Let us now take an integer number $9 > m > 0$, the idea consists in building m linearly independent structural equations by prescribing $E(\phi_{k,i}, i) = 0$ for $k = 1, \cdots, 9-m$ only. It is equivalent to providing the vector's solution of $\mathtt{M}_i[:9-m,:]\mathtt{a}_i[:] = 0$, that is, the vector $\mathtt{a}_i$ belongs to the kernel $\mathcal{K}_i^{\{m\}}$ of the $9-m \times 9$ matrix $\mathtt{M}_i[:9-m,:]$. Since the matrix $\mathtt{M}_i$ is non-singular, the matrix $\mathtt{M}_i[:9-m,:]$ enjoys the maximal rank property, hence the dimension of the kernel is exactly m. The idea consists in building m linearly independent structural equations by determining a basis of the kernel.

2.3. Practical determination of the structural equations

To provide the structural equations with maximal order of accuracy, we proceed in the following way.

- Let $m = 1$ and $\mathcal{K}_i^{\{1\}}$ the kernel of matrix $\mathtt{M}_i[1:8,:]$, we denote by $\mathtt{a}_i^{\{1\}}$ a non-null vector of the kernel and define the coefficients of the structural equation as

  $$a_{i,r}^{\{1\},(s)} = \mathtt{a}_i^{\{1\}}[j], \quad j = j(r,s).$$

  Then the first structural equation $\mathrm{SE1}(i)$ for node i reads

  $$\sum_{r=-1,0,1} \sum_{s=0,1,2} a_{i,r}^{\{1\},(s)} \phi_{i+r}^{(s)} = 0. \tag{10}$$

  By construction, relation (10) provides an eighth-order of consistency in the sense that all the polynomials up to degree 7, exactly match the relation when substituting the approximation with the exact function. Therefore, the rest of the Taylor expansion is in order 8.
- We proceed with $m = 2$ by determining the kernel $\mathcal{K}_i^{\{2\}}$ of the matrix $\mathtt{M}_i[:7,:]$. The subspace is of dimension two and already contains vector $\mathtt{a}_i^{\{1\}}$. We then pick up a second vector $\mathtt{a}_i^{\{2\}}$, orthogonal to $\mathtt{a}_i^{\{1\}}$ to guarantee that the two vectors are linearly independent. The coefficients of the second structural equation $\mathrm{SE2}(i)$ are then defined as

  $$a_{i,r}^{\{2\},(s)} = \mathtt{a}_i^{\{2\}}[j], \quad j = j(r,s),$$

  and the second structural equation just reads

  $$\sum_{r=-1,0,1} \sum_{s=0,1,2} a_{i,r}^{\{2\}(s)} \phi_{i+r}^{(s)} = 0. \tag{11}$$

  Notice that the consistency error is of order 7 since the relation is now exact for polynomial functions up to degree 6.

- The construction of the structural equations for $m = 3$ and higher values is performed inductively. Given the structural equations from 1 to $m-1$, we build the kernel $\mathcal{K}_i^{\{m\}}$ of the matrix $\mathtt{M}_i[:9-m,:]$ and determine an orthogonal vector $\mathtt{a}_i^{\{m\}}$ to the subspace $\mathcal{K}_i^{\{m-1\}}$. We then deduce the m-th structural equation $\mathtt{SEm}(i)$, exact to polynomials up to degree $8-m$.

2.4. Uniform grid case

Assuming that $\Delta x_{i-1/2} = \Delta x_{i+1/2} = \Delta x$, we aim at recovering the relations of the traditional compact scheme, namely the Hermitian case and the combined case. Since the grid is uniform, the coefficients of the structural equations are independent of the node and the functional (9) now reads

$$E(\phi) = \sum_{r=-1,0,1} \sum_{s=0,1,2} a_r^{(s)} \phi^{(s)}(r\Delta x). \tag{12}$$

2.4.1. Hermitian compact equations

The historical design of the Hermitian case is a bit different from the general case, since all the structural equations have the same order. Indeed, the construction is derived from the functional (12) but with additional constraints (see also equations (A.4) and (A.5)). Structural equation SE1 requires that we skip the terms of the second-order derivatives, while we impose $E(\phi_k) = 0$, for $\phi_k = x^0, \cdots, x^4$. We get a system of six unknowns with five linear equations, and the associated one-dimensional kernel provides the non-trivial coefficients for the first Hermitian Structural Equation HSE1 (5).

To provide the second relation, we assume that the coefficients of the first-derivative in (12) are omitted and state $E(\phi_k) = 0$, for $\phi_k = x^0, \cdots, x^4$. We find again that the structural equation from the one-dimensional kernel that provides the second Hermitian Structural Equation HSE2 (6).

The third equation we shall derive is unusual and has not been considered by the traditional Hermitian compact schemes. We assume that the coefficients of the zero-derivative in (12) are omitted, and we build the one-dimensional kernel such that the non-null vector corresponds to the third Hermitian Structural Equation HSE3 given by

$$\frac{D_{i-1} - D_{i+1}}{\Delta x} + \frac{S_{i-1} + 4S_i + S_{i+1}}{3} = 0. \tag{13}$$

Extension to the non-uniform grids is easily achieved by determining the one-dimensional kernels that provide the coefficients of the three structural equations.

The traditional Hermitian method combines the Physical equation PE1 with the two structural equations HSE1 and HSE2. The combination of PE1 with HSE1 and HSE3 or PE1 with HSE2 and HSE3 can be seen as an alternative to the Hermitian scheme, where we directly connect the first derivative to the second derivative. Historically, the compact schemes were elaborated with the following philosophy: All the variables Z, D, S do not have the same "status" and the different authors systematically connect D to Z or S to Z; Variable Z is the reference in the sense that any other variable has to be connected with Z as in (HSE1) and (HSE2).

We claim that there is no reason to privilege Z and all the variables Z D, S should be treated in the same way. In that context, Equation (13) is a relation that does not involve Z and can substitute *HSE*1 or *HSE*2. We have experimented the different combinations (HSE1+HSE3 and HSE2+HSE3) we did not report in the paper since the accuracy is almost the same, so we have decided just to present the alternative HSE3 but without developing the topics. Following the recommendation of the reviewer, we then have added some information about the last equation.

2.4.2. Combined compact equations

The combined compact scheme proposed by P.C. Chu and C. Fan [7] exactly corresponds to the first and second structural equations (7)-(8) provided by the method introduced in subsection 2.3 for the particular case of a uniform grid. The third equation is consistent up to the sixth-order of accuracy CSE3 and, for the uniform grid, reads

$$8\frac{Z_{i+1} - 2Z_i + Z_{i-1}}{\Delta x^2} - 5\frac{D_{i+1} - D_{i-1}}{\Delta x} + (S_{i+1} + S_{i-1}) = 0. \tag{14}$$

2.4.3. An intermediate scheme

The Hermitian scheme requires the introduction of the three quantities Z, D, S but only provides a fourth-order method, whereas the two structural equations are fully implicit, leading to a system with $3 \times (I+1)$ unknowns. To reduce the computational cost using a smaller $2 \times (I+1)$ system, we propose an intermediate scheme by introducing a new structural equation, implicit regarding Z and D but explicit in S.

We first consider the uniform case where analytical expression are simple to derive. To design a relation for S_i regarding Z_{i-1}, Z_i, Z_{i+1}, D_{i-1}, D_i, and D_{i+1}, we assume that $a_{-1}^{(2)} = a_1^{(2)} = 0$ in the functional (12). We then prescribe the six constraints $E(\phi) = 0$, for $\phi = x^0, \cdots, x^5$ for seven unknown coefficients and get, for a uniform grid, the relation

$$S_i = 2\frac{Z_{i-1} - 2Z_i + Z_{i+1}}{(\Delta x)^2} + \frac{D_{i-1} - D_{i+1}}{2\Delta x}, \tag{15}$$

which provides a fourth-order approximation of the second derivative.

We also derive a left-shifted new structural equation between S_{i-1} and the other quantities by assuming that $a_0^{(2)} = a_1^{(2)} = 0$ and using the same constraints $E(\phi) = 0$. We obtain for the uniform grid the relation,

$$S_{i-1} = \frac{-23Z_{i-1} + 16Z_i + 7Z_{i+1}}{2(\Delta x)^2} - \frac{6D_{i-1} + 8D_i + D_{i+1}}{\Delta x}. \tag{16}$$

Similarly, the right-shifted structural equation for S_{i+1} reads

$$S_{i+1} = \frac{-23Z_{i+1} + 16Z_i + 7Z_{i-1}}{2(\Delta x)^2} + \frac{6D_{i+1} + 8D_i + D_{i-1}}{\Delta x}. \tag{17}$$

2.4.4. The intermediate scheme on non-uniform grid

We now consider the general case based on the kernel method where Δx_i is not constant. To derive the relation for S_i, we omit the coefficients $a_{i,-1}^{(2)} = a_{i,1}^{(2)} = 0$ in functional (9). Then, we construct the 7×7 matrix $\mathtt{M}_i$ stating that $E(\phi_{k,i}, i) = 0$ for $k = 0, 1, \cdots, 6$ that involves the seven unknowns. Matrix $\mathtt{M}_i[:6, :]$ has a one-dimensional kernel characterized by the non-null vector which we denote $\mathtt{ac}_i$ and provides the coefficients

$$ac_{i,r}^{(s)} = \mathtt{ac}_i[j], \quad j = j(r,s), \quad r = -1, 0, 1, \quad s = 0, 1.$$

We rescale the eigenvector such that coefficient $ac_{i,0}^{(2)} = 1$. We obtain an explicit relation for S_i labelled Intermediate Centred Structural Equation ICSE(i) at node i of the form

$$S_i = -\sum_{r=-1,0,1} ac_{i,r}^{(0)} Z_{i+r} - \sum_{r=-1,0,1} ac_{i,r}^{(1)} D_{i+r}. \tag{18}$$

Similarly, to provide the relation between S_{i-1} and the other variables D and Z, we omit the coefficients $a_{i,-1}^{(2)} = a_{i,0}^{(2)} = 0$ and build the new matrix $\mathtt{M}$ using the constraints $E(\phi_{k,i}, i) = 0$ for $k = 0, 1, \cdots, 6$. The kernel of matrix $\mathtt{M}_i[:6, :]$ provides the non-null vector, $\mathtt{al}_i$ which we normalize such that $al_{i,-1}^{(2)} = 1$. We then obtain the Intermediate Left-shifted Structural Equation ILSE(i) at node i for S_{i-1} of the form

$$S_{i-1} = -\sum_{r=-1,0,1} al_{i,r}^{(0)} Z_{i+r} - \sum_{r=-1,0,1} al_{i,r}^{(1)} D_{i+r}. \tag{19}$$

At last, a relation for S_{i+1} with respect to the other unknowns is stored in vector $\mathtt{ar}_i$ with normalized coefficient $ar_{i,0}^{(2)} = 1$ and provides the Intermediate Right-shifted Structural Equation at node i IRSE(i)

$$S_{i+1} = -\sum_{r=-1,0,1} ar_{i,r}^{(0)} Z_{i+r} - \sum_{r=-1,0,1} ar_{i,r}^{(1)} D_{i+r}. \tag{20}$$

3. Spectral analysis of the structural equations

Spectral analysis of the structural equation relies on the capacity to resolve the high frequencies for a given grid. Some authors [8,18] present a spectral analysis of the three-points combined compact scheme, while [46] compares classical and compact methods for non-uniform grids. Similarly, in the structural equations we consider the usage of a stencil of three nodes which we assume to be -1, 0 and 1 without losing the generality (a simple shift enables to centre the problem at node 0, thus we skip index i). Moreover, and without loss of generality, we assume that node -1 and node 1 are located at point $x_{-1} = -\Delta x$ and $x_1 = \Delta x$ respectively while node 0 lies in $[-\Delta x, \Delta x]$ with coordinate $x_0 = (2\theta - 1)\Delta x$ as shown in Fig. 1, right panel. For $\theta = 0$ we have $x_0 = x_{-1}$ and $\theta = 1$ corresponds to $x_0 = x_1$. At last $\theta = 0.5$ represents the uniform grid case.

3.1. General spectral equations

Let $\mathrm{i} = \sqrt{-1}$, the imaginary number. Following [29] and [8], we consider the function $\phi(x) = \exp(\mathrm{i}kx)$. The analytical derivatives read $\phi'(x) = \mathrm{i}k\exp(\mathrm{i}kx)$, $\phi''(x) = (\mathrm{i}k)^2\exp(\mathrm{i}kx)$ with $k \in \mathbb{C}$. Structural equations provide approximation of the first and second derivatives, and we write the numerical functions as

$$\begin{aligned} \phi_r^{(1)} &= \mathrm{i}k'\exp(\mathrm{i}kr\Delta x), \qquad k' \in \mathbb{C}, \\ \phi_r^{(2)} &= (\mathrm{i}k'')^2\exp(\mathrm{i}kr\Delta x), \qquad k'' \in \mathbb{C}, \end{aligned}$$

where k' and k'' are some approximations of k for the first and second derivatives respectively. Plug in the approximations $\phi_r^{(0)}$, $\phi_r^{(1)}$, $\phi_r^{(2)}$ in the structural equation with $r = -1, 0, 1$, $s = 0, 1, 2$, provides relations between k, k', k'' and Δx. Roughly speaking, we want that $k' \approx k$ and $k'' \approx k$, that is the ratio k'/k and k''/k has to be close to one. Generally, the authors only consider a uniform grid, but we would like to analyse the spectral resolution even for non-uniform grid.

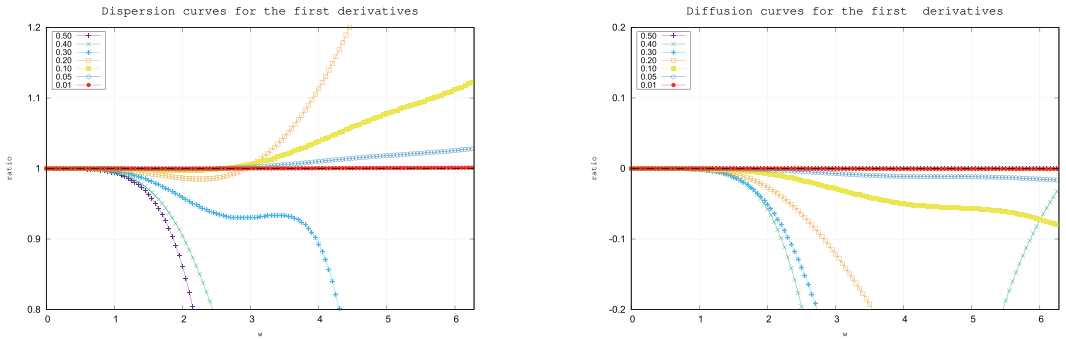

Fig. 2. Dispersion (left panel) and dissipation (right panel) for the first-derivative using the Hermitian scheme. We plot the real and imaginary part of the ratio $\chi'(\omega;\theta)$ in function of ω for several values of θ.

Given θ, we numerically determine the three structural equations (Hermitian, Intermediate or Combined) using the kernel method presented in Section 2.3. To this end, the m-th structural equation SEm is computed, and the Kernel method provides the coefficients $a_r^{\{m\},(s)} = a_r^{\{m\},(s)}(\theta)$, with $r = -1, 0, 1$, $s = 0, 1, 2$. Then, the spectral relations associated to SEm is an expression k' and k'', we write under the form

$$c^{\{m\},(0)} + c^{\{m\},(1)}\,(\mathrm{i}k'\Delta x) + c^{\{m\},(2)}\,(\mathrm{i}k''\Delta x)^2 = 0, \tag{21}$$

where we define for $s = 0, 1, 2$

$$c^{\{m\},(s)}(\omega;\theta) = \sum_{r=-1,0,1} a_r^{\{m\},(s)}(\theta)\exp(\mathrm{i}r\omega), \tag{22}$$

with $\omega = k\Delta x$ and θ the parameter of the grid. At last, noting $\omega' = k'\Delta x$, $\omega'' = k''\Delta x$, a structural equation gives rise to a relation between ω, ω' and ω'' that reads

$$c^{\{m\},(0)}(\omega;\theta) + \mathrm{i}\omega' c^{\{m\},(1)}(\omega;\theta) + (\mathrm{i}\omega'')^2 c^{\{m\},(2)}(\omega;\theta) = 0.$$

Ideally, curves should be $\omega'(\omega;\theta) = \omega$ and $\omega''(\omega;\theta) = \omega$, hence the quality of the formulae regarding the spectral resolution is assessed by the deviation of the ratio

$$\chi'(\omega;\theta) = \frac{\omega'(\omega;\theta)}{\omega},$$
$$\chi''(\omega;\theta) = \frac{\omega''(\omega;\theta)}{\omega}.$$

The closest to unit the coefficients $\chi'(\omega;\theta)$ and $\chi''(\omega;\theta)$ are, the better is the scheme from the spectral point of view. Notice that the real part of corresponds to the dispersion of the scheme, whereas the imaginary part represents the dissipation.

3.2. Hermitian scheme

We begin with the Hermitian case where relation HSE1 connects the function and the first-derivative while $c^{\{1\},(2)}(\omega;\theta) = 0$ leads to the spectral relation

$$c^{\{1\},(0)}(\omega;\theta) + \mathrm{i}\omega' c^{\{1\},(1)}(\omega;\theta) = 0 \tag{23}$$

from which we easily deduce ω' and thus the ratio $\chi'(\omega;\theta)$. We numerically compute χ' and display in Fig. 2 the real part (dispersion) and the imaginary part (dissipation) for several values of θ. Notice that the case $\theta = 1/2$ corresponds to the symmetric case where no dissipation is reported.

Note on the interpretation of the figures. *As we mentioned above, a ratio equal to one represents the ideal situation, hence the curve deviation to the unit quantifies the spectral resolution of the structural equation. Since χ' is a complex value function, the real part and imaginary part represent two distinct aspects of the scheme. The real part relies on the dispersion, that is the phase deviation of the scheme, while the imaginary part is the numerical (anti)diffusion of the scheme. The smaller is the value, the better is the scheme.*

For $\theta \leq 0.1$, we observe a strong improvement of the dispersion and diffusion for the first derivative (the ratio is close to 1 for a longer interval of w).

The second hermitian structural equation HSE2 yields that $c^{\{2\},(1)}(\omega;\theta) = 0$ and provides the spectral equation

$$c^{\{2\},(0)}(\omega;\theta) + (\mathrm{i}\omega'')^2 c^{\{2\},(2)}(\omega;\theta) = 0. \tag{24}$$

We numerically compute the second ratio $\chi''(\omega;\theta)$ and plot in Fig. 3 the dispersion on the left panel and the dissipation on the right panel for the different values of θ.

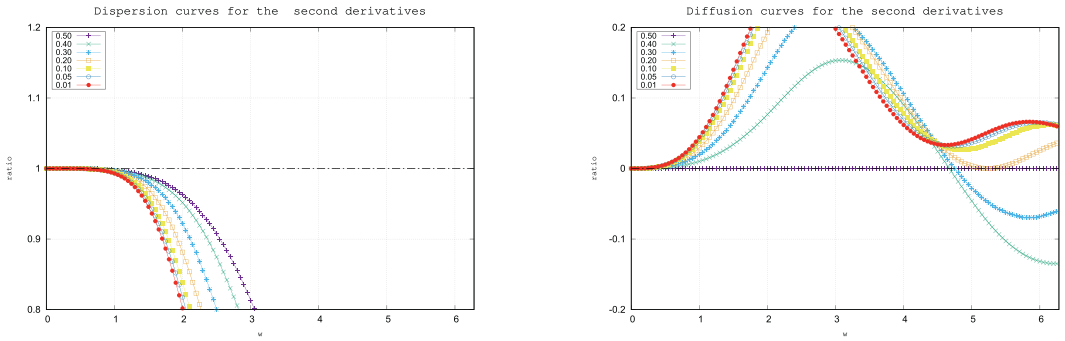

Fig. 3. Dispersion (left panel) and dissipation (right panel) for the second-derivative using the Hermitian scheme. We plot the real and imaginary part of the ratio $\chi''(\omega;\theta)$ in function of ω for several values of θ.

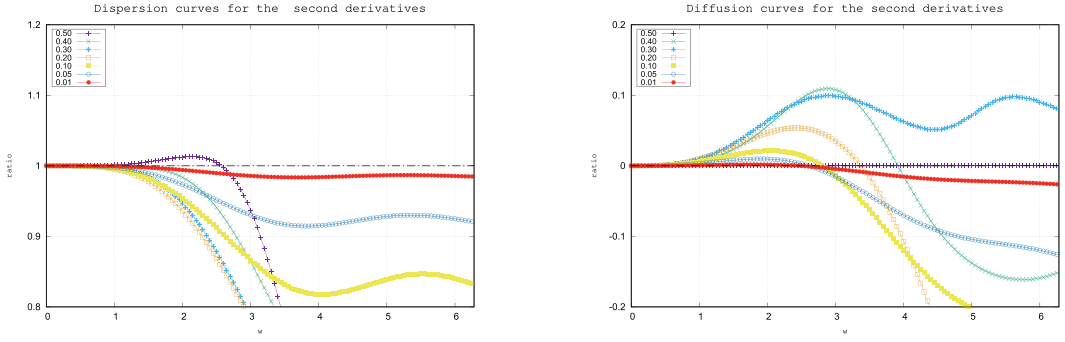

Fig. 4. Dispersion (left panel) and dissipation (right panel) for the second-derivative using the intermediate scheme. We plot the real and imaginary part of the ratio $\chi''(\omega;\theta)$ in function of ω for several values of θ.

The dispersion and dissipation are admissible for $\omega \leq \pi/2$ and the second derivative scheme is far from efficient for larger values, for any values of θ. Such a consequence motivates the adoption of a new representation for the second derivative, implicit in Z and D but explicit in S.

3.3. Intermediate scheme

An upgrade for the second derivative has been proposed with formula (15) in substitution to the original equation (6) in the particular case of a uniform grid. We proceed in the same way for the non-uniform case by substituting HSE2 with ICSE. On the one hand, we use the same spectral equation (23) between the function and the first-derivative but use the intermediate relation (15) with $c^{\{2\},(2)}(\omega;\theta)=1$ and get a modified spectral relation

$$c^{\{2\},(0)}(\omega;\theta)+\mathrm{i}\omega' c^{\{2\},(1)}(\omega;\theta)+(\mathrm{i}\omega'')^2=0. \tag{25}$$

Plugging the expression of ω' from (23) into relation (25) provides a relation of ω'' regarding ω, thus $\chi''(\omega;\theta)$. We plot in Fig. 4 the dispersion (left panel) and the dissipation (right panel) for the ratio. The gain of spectral resolution for the second derivative is noticeable compared to the Hermitian case (24). In particular, small values of θ enable to achieve excellent spectral properties both for the dispersion and the dissipation.

3.4. Combined schemes

The Combined scheme fully couples the function and its derivatives, leading to a more expensive system to solve. However, it provides the best spectral resolution. Gathering the two structural equations CSE1 and CSE2 yields

$$0=c^{\{1\},(0)}(\omega;\theta)+\mathrm{i}\omega' c^{\{1\},(1)}(\omega;\theta)+(\mathrm{i}\omega'')^2 c^{\{1\},(2)}(\omega;\theta),$$
$$0=c^{\{2\},(0)}(\omega;\theta)+\mathrm{i}\omega' c^{\{2\},(1)}(\omega;\theta)+(\mathrm{i}\omega'')^2 c^{\{2\},(2)}(\omega;\theta).$$

Solving the 2×2 linear system in order to ω' and ω'' provides the ratio $\chi'(\omega;\theta)$ and $\chi''(\omega;\theta)$. We plot in Fig. 5 the ratio for the first derivative with the respective dispersion and dissipation, while the spectral resolution of the second derivative approximation is given in Fig. 6.

The curves clearly suggest that the dispersion and dissipation are strongly reduced for small values of θ. It indicates that a grid constituted of a series of pairs of close points of the form $x_{2i}=i\Delta x$, $x_{2i+1}=x_{2i}+\theta\Delta x$ with a small θ would be efficient to catch high-frequency plane waves.

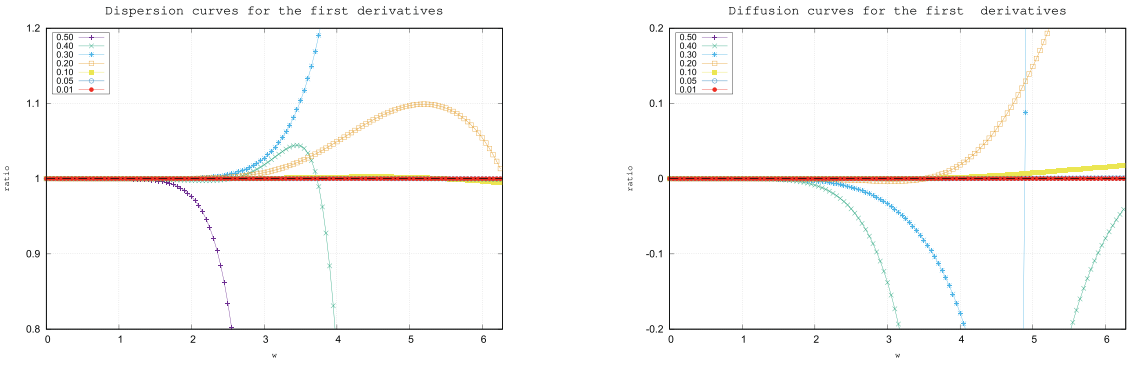

Fig. 5. Dispersion (left panel) and dissipation (right panel) for the first-derivative using the combined scheme. We plot the real and imaginary part of the ratio $\chi'(\omega;\theta)$ in function of ω for several values of θ.

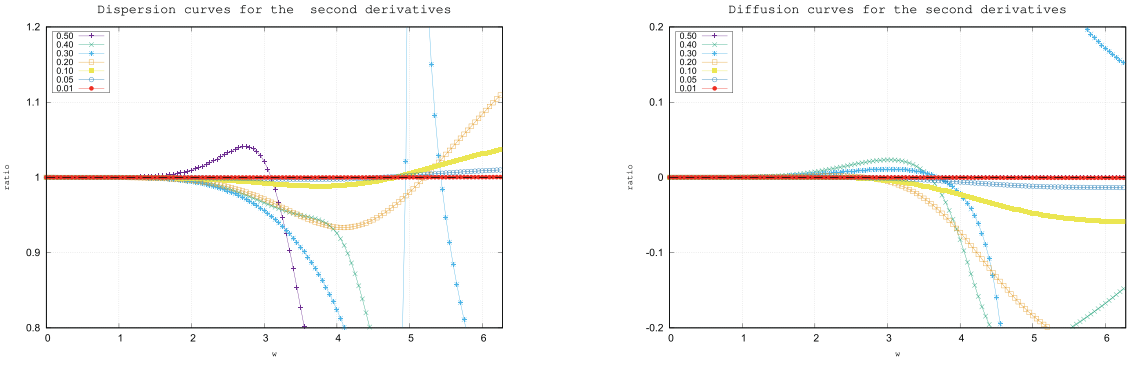

Fig. 6. Dispersion (left panel) and dissipation (right panel) for the second-derivative using the combined scheme. We plot the real and imaginary part of the ratio $\chi''(\omega;\theta)$ in function of ω for several values of θ.

4. The numerical schemes

We design two numerical schemes by combining the structural and the physical equations. The boundary conditions are treated similarly to the inner domain problem, namely the boundary equation corresponds to an additional physical equation PE2 while we shall use a specific structural equation to take the one-side configuration of the border.

To provide a guideline for the presentation, we consider the simple linear convection diffusion equation given by

$$-\kappa\phi'' + u\phi' = f \tag{26}$$

with $\kappa \geq 0$ the diffusion coefficient, u the velocity, while f stands for the source term. The domain is the interval $\Omega = [x_L, x_R]$ and we prescribe general Robin boundary conditions on the left and right side $x_L = 0$ and $x_R = 1$ as

$$\alpha_L\phi(x_L) + \beta_L\phi'(x_L) = g_L, \tag{27}$$

$$\alpha_R\phi(x_R) + \beta_R\phi'(x_R) = g_R. \tag{28}$$

4.1. Scheme 4thZD

The fourth-order scheme is obtained by combining the structural equation HSE1 and the intermediate structural equation ICSE for the second derivative for inner nodes, while we take the relations ILSE and IRSE for the left and right boundary nodes. The scheme is designed as follows.

- Inner nodes $i = 1, \cdots, I-1$:
  We use the physical equation PE1(i): $-\kappa S_i + uD_i = f_i$ together with HSE1(i) and ICSE(i).
- Left node $i = 0$:
  We use again the physical equation PE1(0): $-\kappa S_0 + uD_0 = f_0$ together with the ILSE(1) **at node** $i = 1$ to provide a non-trivial relation for S_0. We add the other physical equation PE2(0): $\alpha_L Z_0 + \beta_L D_0 = g_L$ that prescribes the boundary condition.

- Right node $i = I$:
  Similarly, we take the physical equation PE1(I): $-\kappa S_I + uD_I = f_I$ together with the IRSE($I-1$) **at node** $i = I-1$ to involve S_I. The other boundary physical equation PE2(I) then reads $\alpha_R Z_I + \beta_R D_R = g_R$.

  The assembly matrix has the following structure

$$\begin{bmatrix} \text{PE1(0)} & & & & & \\ \text{PE2(0)} & & & & & \\ \text{ILSE(0)} & & & & & \\ & \ddots & & & & \\ & & \text{PE1(i)} & & & \\ & & \text{HSE1(i)} & & & \\ & & \text{ICSE(i)} & & & \\ & & & \ddots & & \\ & & & & \text{PE1(I)} & \\ & & & & \text{PE2(I)} & \\ & & & & \text{IRSE(I)} & \end{bmatrix} \begin{bmatrix} Z_0 \\ D_0 \\ S_0 \\ \vdots \\ Z_i \\ D_i \\ S_i \\ \vdots \\ Z_I \\ D_I \\ S_I \end{bmatrix} = \begin{bmatrix} f_0 \\ g_L \\ 0 \\ \vdots \\ f_i \\ 0 \\ 0 \\ \vdots \\ f_I \\ g_R \\ 0 \end{bmatrix}.$$

Since the relation ILSE, ICSE and IRSE are explicit regarding S, the system is reshaped into a $2(I+1)$ system by substituting S_i with its representation. Consequently, the solution just involves the data $(Z_i, D_i)_{i=0}^{I}$ and approximations of S_i are computed *a posteriori* with the Intermediate relations ICSE, ILSE and IRSE.

4.2. Scheme 6thZDS

The sixth-order scheme has some similarities with the original combined compact scheme of Chu and Fan [7] but differs in several points: (i) we use the third structural equation for the boundary condition treatment; (ii) we derive the structural equations using the computation of the different kernels using $m = 1, 2$ and 3 deriving from matrix $\mathtt{M}_i$ that give more versatility to provide the structural equations when dealing with non-uniform grids. The design of the scheme is as follows.

- Inner nodes $i = 1, \cdots, I-1$:
  We use the physical equation PE1(i): $-\kappa S_i + uD_i = f_i$ together with equation CSE1(i) and CSE2(i).
- Left node $i = 0$:
  We use the physical equation PE1(0): $-\kappa S_0 + uD_0 = f_0$ and the boundary condition PE2(0): $\alpha_L Z_0 + \beta_L D_0 = g_L$ that provides the boundary condition. At last, the structural equation CSE3(1) (**note that the index is 1, and not 0**) closes the system.
- Right node $i = I$:
  Similarly, the physical equations PE1(I): $-\kappa S_I + uD_I = f_I$ and PE2(I): $\alpha_R Z_I + \beta_R D_I = g_R$ provide the boundary condition. At last, the structural equation CSE3($I-1$) (**note that the index is I-1, and *NotI***) closes the system.

  The structure of the linear system reads,

$$\begin{bmatrix} \text{PE1(0)} & & & & & \\ \text{PE2(0)} & & & & & \\ \text{CSE3(1)} & & & & & \\ & \ddots & & & & \\ & & \text{PE1(i)} & & & \\ & & \text{CSE1(i)} & & & \\ & & \text{CSE2(i)} & & & \\ & & & \ddots & & \\ & & & & \text{PE1(I)} & \\ & & & & \text{PE2(I)} & \\ & & & & \text{CSE3(I-1)} & \end{bmatrix} \begin{bmatrix} Z_0 \\ D_0 \\ S_0 \\ \vdots \\ Z_i \\ D_i \\ S_i \\ \vdots \\ Z_I \\ D_I \\ S_I \end{bmatrix} = \begin{bmatrix} f_0 \\ g_L \\ 0 \\ \vdots \\ f_i \\ 0 \\ 0 \\ \vdots \\ f_I \\ g_R \\ 0 \end{bmatrix}.$$

Remark. Notice that we are expecting a fifth-order scheme due to the use of the structural equation CSE3 at the boundary. On the one hand, we lose accuracy, but on the other hand, we do not need to introduce a more complex structural equation involving other nodes. □

5. Benchmarking

We carry out several benchmarks to assess the accuracy, stability and spectral precision of the method together with the ability to handle non-linear problems. Since we are dealing with regular solutions, we use the L^∞-norm of the error of the

Table 1
Errors and convergence orders for scheme 4thZD.

	uniform		non-uniform		
I	error Z	order	error Z	order	σ
10	8.64e-06	***	1.30e-05	***	2.62e-06
20	6.52e-07	3.7	7.67e-07	4.1	1.60e-07
40	4.55e-08	3.8	5.05e-08	3.9	5.93e-09
80	3.02e-09	3.9	3.36e-09	4.0	3.13e-10
	uniform		non-uniform		
I	error D	order	error D	order	σ
10	4.41e-04	***	3.70e-04	***	1.25e-04
20	2.98e-05	3.9	2.87e-05	3.7	6.95e-06
40	1.94e-06	3.9	2.00e-06	3.8	7.90e-07
80	1.24e-07	4.0	1.39e-07	3.9	5.92e-08
	uniform		non-uniform		
I	error S	order	error S	order	σ
10	4.41e-04	***	3.70e-04	***	1.25e-04
20	2.98e-05	3.9	2.87e-05	3.7	6.95e-06
40	1.94e-06	3.9	2.00e-06	3.8	7.90e-07
80	1.24e-07	4.0	1.39e-07	3.9	5.92e-08

solution over the grid $G = (x_i)_{i=0}^{I}$, given by

$$E_Z(G) = \max_{x_i \in G} |Z_i - \phi(x_i)|.$$

The method order between two consecutive grids is given by

$$O_Z(G, G') = \frac{\ln\left(E_Z(G)/E_Z(G')\right)}{\ln\left(|G'|/|G|\right)}$$

where $|G|$ is the number of points of the grid. Similarly, we define E_D, O_D and E_S, O_S to assess the first and second derivative convergence order.

5.1. Convection diffusion equation

We are concerned with the accuracy of the simple convection diffusion problem. Such a problem is an important building-block to solving non-linear problems in the future and has been studied by a large community of researchers. In [52] (see also [57]), the authors apply a fourth-order HODIE formulation for the Poisson equation, while [24] use the standard Hermitian compact scheme for non-linear diffusion equations.

We seek the numerical approximation of

$$-\kappa\phi'' + v\phi' = f \tag{29}$$

on the [0,1] interval with $\kappa > 0$ and $v \in \mathbb{R}$ while f stands for the source term. We test two kinds of boundary conditions and check the accuracy.

5.1.1. Dirichlet-Dirichlet boundary conditions

We first prescribe Dirichlet condition on both sides of the domain. The manufactured solution is $\phi(x) = \exp(2x)$ and the right-hand side f is computed to match the physical equation. We take $\kappa = 1$, $v = 1$ and carry out the calculation of the errors and orders for different values of I.

We present in Tables 1 and 2 the errors and convergence orders for the 4thZD and 6thZDS schemes, respectively. To assess the accuracy with non-uniform grid, we carry out 10 times the simulation with random deformed grids by moving arbitrary the inner nodes to up 30% of the original uniform grid. We provide the statistics (average and standard deviation σ) to compare with the uniform grid case. We obtain the optimal accuracy for the fourth-order scheme, while the 6thZDS scheme only achieves the sixth-order of accuracy for the approximation Z. The accuracy of the first and second derivative is degraded, and we report a fifth-order of convergence.

5.1.2. Dirichlet-Neumann boundary conditions

We use again the manufactured solution $\phi(x) = \exp(2x)$ and prescribe the Neumann condition $\phi'(0) = -2$ on the left side, while the Dirichlet condition $\phi(1) = e^2$ is imposed on the right side. The Source term f is deduced from the exact solution, and we take $\kappa = 1$, $v = 1$. We apply the 4thZD and 6thZDS schemes using a uniform grid of $I + 1$ points. We also

Table 2
Errors and convergence orders for scheme `6thZDS`.

	uniform		non-uniform		
I	error Z	order	error Z	order	σ
10	1.06e-06	***	1.07e-06	***	5.66e-07
20	1.96e-08	5.8	2.55e-08	5.4	1.12e-08
40	3.34e-10	5.9	6.20e-10	5.5	2.57e-10
80	5.36e-12	6.0	9.58e-12	6.0	4.93e-12
	uniform		non-uniform		
I	error D	order	error D	order	σ
10	4.70e-05	***	4.01e-05	***	1.50e-05
20	2.98e-05	4.8	1.61e-06	4.6	4.56e-06
40	5.40e-08	4.9	5.70e-08	4.8	2.03e-08
80	1.72e-09	5.0	1.96e-09	4.9	8.36e-10
	uniform		non-uniform		
I	error S	order	error S	order	σ
10	4.70e-05	***	4.01e-05	***	1.50e-05
20	2.98e-05	4.8	1.61e-06	4.6	4.56e-06
40	5.40e-08	4.9	5.70e-08	4.8	2.03e-08
80	1.72e-09	5.0	1.96e-09	4.9	8.36e-10

Table 3
Errors and convergence orders for `4thZD`.

	Uniform		non-uniform		
I	error Z	order	error Z	order	σ
10	1.90e-04	***	2.11e-04	***	4.93e-05
20	1.19e-05	4.0	1.39e-05	3.9	6.32e-06
40	7.46e-07	4.0	7.63e-07	4.2	1.09e-07
80	4.67e-08	4.0	5.39e-08	3.8	1.86e-08
	Uniform		non-uniform		
I	error D	order	error D	order	σ
10	5.25e-04	***	5.52e-04	***	1.09e-04
20	3.48e-05	3.9	3.98e-05	3.8	1.01e-05
40	2.24e-06	3.9	2.31e-06	4.1	2.34e-07
80	1.42e-07	4.0	1.64e-07	3.8	3.05e-08
	Uniform		non-uniform		
I	error S	order	error S	order	σ
10	5.25e-04	***	5.52e-04	***	1.09e-04
20	3.48e-05	3.9	3.98e-05	3.8	1.01e-05
40	2.24e-06	3.9	2.31e-06	4.1	2.34e-07
80	1.42e-07	4.0	1.64e-07	3.8	3.05e-08

generate non-uniform grids by applying a 30% perturbation to the inner nodes to assess the convergence for mild deformed grids. We report the errors and convergence order in Tables 3 and 4 for the fourth and fifth order schemes, respectively. We compute 10 times the solution and errors with different deformed grids and report the statistics to compare with the uniform grid case.

We obtain an effective fourth-order of accuracy with `4thZD` and a fifth-order for scheme `6thZDS` due to the Neumann boundary condition. We observe a significant error reduction of two orders of magnitude between the schemes (for instance, E_Z with $I = 80$). As indicated, the boundary treatment is simply achieved by combining the two Physical Equations (convection diffusion and the boundary condition) with the third structural equation. Notice that the error for the first and second derivative are the same, due to the physical equation that directly links D to S.

5.1.3. Boundary layer

A critical issue for convection diffusion problem is the boundary layers that represent a challenging question to correctly catch the strong gradients near the boundary. We consider the equation $-\kappa\phi'' + v\phi' = f$ with $f = 0$ and the boundary conditions $\phi(0) = 1$ and $\phi(1) = 0$ such that we develop a boundary layer on the right side $x_R = 1$. The exact solution is given by

$$\phi(x) = \frac{\exp(v/\kappa) - \exp(vx/\kappa)}{\exp(v/\kappa) - 1}$$

Table 4
Errors and convergence orders for 6thZDS.

	Uniform		non-uniform		
I	error Z	order	error Z	order	σ
10	1.74e-05	***	2.35e-05	***	1.04e-05
20	4.84e-07	5.1	4.49e-07	5.7	2.57e-07
40	1.42e-08	5.0	1.80e-08	4.6	1.15e-08
80	4.29e-10	5.0	4.46e-10	5.3	2.41e-10
	Uniform		non-uniform		
I	error D	order	error D	order	σ
10	7.44e-05	***	8.77e-05	***	2.71e-05
20	2.40e-06	4.9	2.08e-06	5.4	8.33e-07
40	7.65e-08	5.0	9.31e-08	4.5	3.81e-08
80	2.40e-09	5.0	2.26e-09	5.4	8.06e-10
	Uniform		non-uniform		
I	error S	order	error S	order	σ
10	7.44e-05	***	8.77e-05	***	2.71e-05
20	2.40e-06	4.9	2.08e-06	5.4	8.33e-07
40	7.65e-08	5.0	9.31e-08	4.5	3.81e-08
80	2.40e-09	5.0	2.26e-09	5.4	8.06e-10

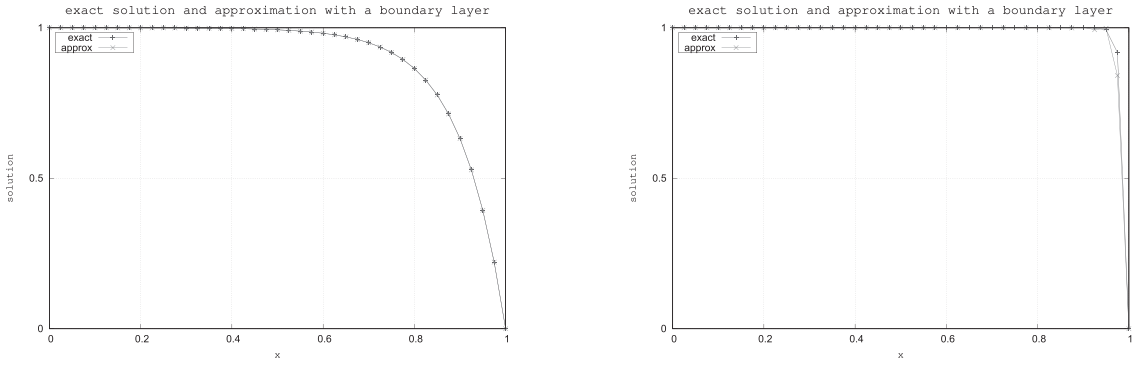

Fig. 7. Solution of the boundary layer problem for $Pe = 10$ (left panel) and $Pe = 100$ (right panel) with a grid of $I = 80$ points. The characteristic size of the boundary layer is e/Pe.

For $\kappa = 0.1$ and $v = 1$ (Péclet number $Pe = 10$), we obtain a mild boundary layer of characteristic length $h = e/Pe$, $e = \exp(1)$ which we easily catch with a $I = 80$ uniform grid Fig. 7, left panel). Taking $\kappa = 0.01$ and $u = 1$ yields to a more difficult approximation of the boundary layer with a strong local gradient (Fig. 7, right panel). We observe that no oscillations are created even in the situation $\Delta x > e/Pe$ that usually provokes undesirable non-physical oscillations.

We report in Table 5 the relative errors (by dividing with the maximum value) and convergence orders, both for schemes 4thZD and 6thZDS for the Péclet number $Pe = 100$. The coarsest grid $I = 40$ enables to catch the steep gradient with the two schemes. The fourth-order scheme reaches to the asymptotic optimal order, but the 6thZDS scheme requires finer grids to recover the asymptotic sixth-order of convergence for the function. Notice that the first and second derivatives only converge to a fifth-order of accuracy.

5.2. Helmholtz equation

Helmholtz's equation is a standard benchmark for evaluating the dispersion of a numerical method and the phase alteration [53]. We consider the linear complex value problem on the domain [0,1]

$$-\phi'' + (2\pi k)^2\phi = f \tag{30}$$

equipped with the boundary conditions $\phi(0) = 0$ and the Sommerfeld radiation condition [13] expressed by $\phi'(1) - \mathrm{i}2\pi k\phi(1) = 0$. The exact complex solution is given by $\phi(x) = \exp(\mathrm{i}2\pi kx)$ with $f = 0$. We use $I = 80$ in all the cases and carry out the simulations for different wave numbers k. The relative errors for the first and second derivatives are obtained by dividing the absolute error with $2\pi k$ and $(2\pi k)^2$ respectively to draw a fair comparison for the different wave numbers.

Table 6 reports the relative error of the two schemes for the function, the first and second derivative, regarding the frequency. Since $I = 80$, the maximum wave number is $k = 25$ and corresponds to $\omega = 2\pi 25$, $\Delta x = \frac{25}{40}\pi \approx 1.96$ to confront with the spectral curves of Section 3. As expected, the scheme 6thZDS provides better accuracy. Nevertheless, the errors

Table 5
Relative errors and convergence orders for the boundary layer problem ($Pe = 100$) using `4thZD` (left table) and `6thZDS` (right table).

	4thZD					
I	error Z	order	error S	order	error D	order
40	7.67e-02	***	1.62e-01	***	1.62e-01	***
80	3.89e-03	4.3	1.73e-02	3.2	1.73e-02	3.2
160	3.39e-04	3.5	1.61e-03	3.4	1.61e-03	3.4
320	2.38e-05	3.8	1.27e-04	3.7	1.27e-04	3.7
640	1.63e-06	3.9	8.95e-06	3.8	8.95e-06	3.8
	6thZDS					
I	error Z	order	error S	order	error D	order
40	8.25e-03	***	1.30e-01	***	1.30e-01	***
80	6.38e-04	3.7	1.01e-02	3.7	1.01e-02	3.7
160	4.61e-05	3.8	5.85e-04	4.1	5.85e-04	4.1
320	1.48e-06	5.0	2.58e-05	4.5	2.58e-05	4.5
640	1.96e-08	6.2	8.88e-07	4.9	8.88e-07	4.9

Table 6
Relative errors for the `4thZD` (left panel) and `6thZDS` scheme (right panel) with $I = 80$ points.

	4thZD		
k	error Z	error D	error S
2.0	1.41e-05	1.86e-05	1.41e-05
6.0	1.07e-03	1.24e-03	1.07e-03
10.0	7.72e-03	8.15e-03	7.72e-03
15.0	3.60e-02	3.66e-02	3.60e-02
20.0	1.04e-01	1.09e-01	1.04e-01
25.0	2.33e-01	2.49e-01	2.33e-01
	6thZDS		
k	error Z	error D	error S
2.0	1.14e-06	1.36e-06	1.14e-06
6.0	2.06e-04	2.72e-04	2.06e-04
10.0	3.12e-03	3.13e-03	3.12e-03
15.0	2.15e-02	2.20e-02	2.15e-02
20.0	8.49e-02	8.65e-02	8.49e-02
25.0	2.38e-01	2.48e-01	2.38e-01

between the two methods tend to be very similar for the highest frequencies. Spectral resolution is excellent and numerical simulations confirm the theoretical study.

5.3. Viscous burger's equation

The non-linear Bürger's equation is a popular benchmark for assessing the numerical scheme for a non-linear problem within a simple context. Liao [30] proposed a fourth HODIE formulation for the non-stationary 1D case, and an extension for the sixth-order was proposed in [47] (see also [56]). We also mention that a WENO version has been developed in [23] for the non-regular case when solutions present some discontinuity in space (see also [15] for implicit method with conservation law).

We seek a solution on $\Omega = [0, 1]$ for the problem

$$\phi\phi' - \varepsilon\phi'' = f,$$

with $\varepsilon \geq 0$ the dissipation coefficient. Adopting the $Z - D - S$ notation, the equation reads $ZD - \varepsilon S = f$ and clearly highlights the non-linearity resulting from the product ZD. To this end, one has to introduce some iterative procedure and linearize the equation. We seek a sequence $(Z^{(k)}, D^{(k)}, S^{(k)})$, $k = 0, \cdots,$ by solving successively: given $Z^{(k)}$, compute $Z^{(k+1)}$, $D^{(k+1)}$, $S^{(k+1)}$ such as

$$Z^{(k)}D^{(k+1)} - \varepsilon S^{(k+1)} = f,$$

with the appropriate boundary conditions.

At the discrete level, we denote by $Z = [Z_0, \cdots, Z_I]^{\,t}$ the approximation of $\phi(x_i)$, over the grid x_i, $i = 0, \cdots, I$ and similar notations are adopted for D and S. Noting that $Z^{(k)}$ plays the role of the velocity in equation (29), we just have to update the velocity and solve the linear system. Notice that the velocity varies in space. We now detail the two schemes.

Table 7
Errors and convergence orders for the viscous Burger equation with scheme 4thZD.

	uniform		non-uniform		
I	error Z	order	error Z	order	σ
40	2.08E-04	***	4.42E-03	***	2.75E-03
80	1.57E-05	3.7	1.57E-04	4.8	1.12E-04
160	1.01E-06	4.0	6.30E-06	4.6	3.77E-06
320	6.34E-08	4.0	1.52E-07	5.4	7.85E-08
640	3.96E-09	4.0	1.33E-08	3.5	7.00E-09
	uniform		non-uniform		
I	error D	order	error D	order	σ
40	5.67E-03	***	6.83E-03	***	7.79E-04
80	3.24E-04	4.1	3.78E-04	4.2	4.39E-05
160	1.97E-05	4.0	2.53E-05	3.9	2.73E-06
320	1.23E-06	4.0	1.56E-06	4.0	1.03E-07
640	7.69E-08	4.0	1.00E-07	4.0	4.63E-09
	uniform		non-uniform		
I	error S	order	error S	order	σ
40	2.73E-06	***	1.34E-04	***	8.81E-05
80	2.18E-07	3.7	4.77E-06	4.8	3.55E-06
160	1.41E-08	4.0	1.66E-07	4.8	1.16E-07
320	8.81E-10	4.0	3.90E-09	5.4	1.86E-09
640	5.65E-11	4.0	3.72E-10	3.4	2.18E-10

- The 4thZD scheme combines the physical equation PE1(i)

$$Z_i^{(k)} D_i^{(k+1)} - \varepsilon S_i^{(k+1)} = f_i, \quad i = 1, \cdots, I-1$$

with the structural equation HSE1(i) for the first derivative and ICSE(i) for the second derivative. The Dirichlet boundary conditions are treated as indicated in the Dirichlet-Dirichlet situation for the linear case with $i = 0$ and $i = I$.
- The 6thZDS scheme uses the same physical equation together with the two structural equations CSE1(i) and CSE2(i). One more time, the boundary conditions are similarly treated with the additional physical equation and the CSE3(i) relation for $i = 0$ and $i = I$.

To assess the accuracy of the scheme, we use the manufactured solution

$$\phi(x) = \frac{1}{1 + 100(x - 1/2)^2}$$

and prescribe the Dirichlet condition on both sides of the domain. The source term f is computed by applying the viscous Burger equation to the exact solution with $\epsilon = 1$.

Table 7 provides the absolute errors and convergence rates for the 4thZD scheme. We present two situations: the uniform grid and the deformed grid by using a 30% random perturbation of the uniform grid. We report the statistics based on 10 samples. We clearly find out the fourth-order of accuracy both for the function and the successive derivatives. Table 8 corresponds to the errors for the 6thZDS scheme. For the coarser grid, the order of convergence is optimal and corresponds to the expected one. Nevertheless, the error reduction is stuck to 1.0E-11 due to the high conditioning number of the system.

5.4. Isentropic euler system

We now deal with the 1D isentropic Euler problem, given by the following non-linear hyperbolic system over domain $\Omega =]x_L, x_R[$, with ρ the density, u the velocity and $p = \kappa \rho^\gamma$ the pressure with $\kappa > 0$ and $\gamma \in]1, 3[$

$$A(x) = \rho \frac{du}{dx} + u \frac{d\rho}{dx},$$
$$B(x) = \rho u \frac{du}{dx} + \frac{dp}{dx}.$$

Source terms $A(x)$ and $B(x)$ are given functions together with the Dirichlet condition for ρ and u at the boundaries $x = x_L$ and x_R. We introduce the variables Z_ρ, D_ρ, Z_u, and D_u as the approximations at the grid nodes of ρ, ρ', u and u' respectively. The system then reads

$$A(x) = Z_\rho D_u + Z_u D_\rho,$$
$$B(x) = Z_\rho Z_u D_u + \kappa \gamma (Z_\rho)^{\gamma - 1} D_\rho.$$

Table 8
Errors and convergence orders for the viscous Burger equation with scheme `6thZDS`.

	uniform		non-uniform		
I	error Z	order	error Z	order	σ
40	4.47E-05	***	1.2E-03	7.3	6.88E-04
80	7.31E-07	5.9	7.81E-06	7.3	6.81E-06
160	1.25E-08	5.9	1.12E-07	6.1	9.52E-08
320	1.15E-09	3.4	9.42E-10	6.9	3.40E-10
640	1.98E-09	-0.8	7.96E-11	3.6	4.49E-11
	uniform		non-uniform		
I	error D	order	error D	order	σ
40	8.51E-04	***	1.35E-03	***	3.48E-04
80	1.03E-05	6.4	1.48E-05	6.5	2.89E-06
160	1.51E-07	6.1	2.74E-07	5.8	7.80E-08
320	1.59E-09	6.6	4.21E-09	6.0	2.82E-10
640	4.80E-09	-1.6	7.49E-11	5.8	1.36E-11
	uniform		non-uniform		
I	error S	order	error S	order	σ
40	8.53E-07	***	3.81E-05	***	2.24E-05
80	1.09E-08	6.3	2.41E-07	7.3	2.04E-07
160	1.38E-10	6.3	3.24E-09	6.2	2.87E-09
320	3.48E-11	2.0	2.64E-11	6.9	1.04E-11
640	6.04E-11	-0.8	2.42E-12	3.4	1.41E-12

To overcome the non-linearity issue, we propose two types of linearization we shall compare in terms of stability and computational efficiency. The linearization is based on an iterative procedure where one as to build a succession $\left(Z_\rho^{(k)}, D_\rho^{(k)}, Z_u^{(k)}, D_u^{(k)}\right)$ that converges to the solution $(\overline{Z}_\rho, \overline{D}_\rho, \overline{Z}_u, \overline{D}_u)$ of the non-linear discrete problem.

5.4.1. Rough linearization

Let us assume that we have an approximation at iteration k. The rough linearization simply consists of substituting most of the terms with their approximation at stage k and keeping the most predominant terms for the solver stage $k+1$.

$$A(x) = D_u^{(k)} Z_\rho^{(k+1)} + Z_u^{(k)} D_\rho^{(k+1)}, \tag{31}$$

$$B(x) = Z_\rho^{(k)} Z_u^{(k)} D_u^{(k+1)} + \kappa\gamma\left(Z_\rho^{(k)}\right)^{\gamma-1} D_\rho^{(k+1)}. \tag{32}$$

For the mass conservation, we have privileged the density variable, while the momentum conservation equation focuses on the velocity variable.

5.4.2. Upgrade of the pressure discretisation

Pressure represents the major non-linearity in the Euler system and may lead to non-physical oscillations. To this end, we propose a better discretisation for $(Z_\rho)^{\gamma-1} D_\rho$. Let $Z_\rho^{(k)}$ and $Z_\rho^{(k+1)}$ be the two successive stages, one has

$$\begin{aligned}\left(Z_\rho^{(k+1)}\right)^{\gamma-1} &= \left(Z_\rho^{(k+1)} - Z_\rho^{(k)} + Z_\rho^{(k)}\right)^{\gamma-1},\\ &\approx \left(Z_\rho^{(k)}\right)^{\gamma-1} + (\gamma-1)\left(Z_\rho^{(k)}\right)^{\gamma-2}\left(Z_\rho^{(k+1)} - Z_\rho^{(k)}\right)\\ &\approx (2-\gamma)\left(Z_\rho^{(k)}\right)^{\gamma-1} + (\gamma-1)\left(Z_\rho^{(k)}\right)^{\gamma-2} Z_\rho^{(k+1)}.\end{aligned}$$

We then propose the linearization

$$\left(\frac{dp}{dx}\right)^{(k+1)} \approx \kappa\gamma(2-\gamma)\left(Z_\rho^{(k)}\right)^{\gamma-1} D_\rho^{(k+1)} + \kappa\gamma(\gamma-1)\left(Z_\rho^{(k)}\right)^{\gamma-2} Z_\rho^{(k+1)} D_\rho^{(k)}$$

and substitute in place of $\kappa\gamma\left(Z_\rho^{(k)}\right)^{\gamma-1} D_\rho^{(k+1)}$ providing the relation

$$B(x) = Z_\rho^{(k)} Z_u^{(k)} D_u^{(k+1)} + \kappa\gamma(2-\gamma)\left(Z_\rho^{(k)}\right)^{\gamma-1} D_\rho^{(k+1)} + \kappa\gamma(\gamma-1)\left(Z_\rho^{(k)}\right)^{\gamma-2} Z_\rho^{(k+1)} D_\rho^{(k)}. \tag{33}$$

Table 9
Relative errors and convergence orders for the Isentropic Euler Problem using 4thZD and 6thZDS using the rough linearization.

	4thZD								
I	error u	order	error ρ	order	error u'	order	error ρ'	order	its
20	2.76e-08	***	1.11e-09	***	5.19e-09	***	6.58e-09	***	72
40	1.88e-09	3.9	7.54e-11	3.9	3.66e-10	3.9	4.30e-10	3.9	72
80	1.23e-10	3.9	5.00e-12	3.9	2.47e-11	3.9	2.76e-11	4.0	71
160	8.06e-12	3.9	3.90e-13	3.7	2.98e-12	3.1	1.78e-12	4.0	71

	6thZDS												
I	error u	order	error ρ	order	error u'	order	error ρ'	order	error u''	order	error ρ''	order	its
10	1.90e-09	***	1.08e-09	***	1.01e-08	***	6.57e-09	***	1.99-06	***	1.89e-06	***	69
20	3.98e-11	5.6	2.36e-11	5.5	2.42e-10	5.4	1.42e-10	5.5	1.53e-07	3.7	1.42e-07	3.7	69
30	4.31e-12	5.5	2.36e-12	5.7	2.44e-11	5.7	1.40e-11	5.7	3.46e-08	3.7	2.99e-08	3.9	69
40	1.29e-12	4.2	4.62e-13	5.7	6.02e-12	4.9	2.67e-12	5.8	1.34e-08	3.3	9.72e-09	3.9	70

Table 10
Relative errors and convergence orders for the Isentropic Euler Problem using 4thZD and 6thZDS using the upgraded linearization.

	4thZD								
I	error u	order	error ρ	order	error u'	order	error ρ'	order	its
20	2.76e-08	***	1.11e-09	***	5.19-09	***	6.58e-09	***	70
40	1.88e-09	3.9	7.54e-11	3.9	3.66e-10	3.9	4.30e-10	3.9	71
80	1.23e-10	3.9	5.05e-12	3.9	2.47e-11	3.9	2.76e-11	4.0	70
160	8.12e-12	3.9	4.35e-13	3.5	2.69e-12	3.2	1.80e-12	3.9	71

	6thZDS												
I	error u	order	error ρ	order	error u'	order	error ρ'	order	error u''	order	error ρ''	order	its
10	1.96e-09	***	1.08e-09	***	1.07e-08	***	6.57e-09	***	2.04e-06	***	1.89e-06	***	70
20	4.07e-11	5.6	2.36e-11	5.5	2.59e-10	5.4	1.42e-10	5.5	1.57e-07	3.7	1.42e-07	3.7	70
30	4.25e-12	5.6	2.34e-12	5.7	2.85e-11	5.4	1.39e-11	5.7	3.48e-08	3.7	2.99e-08	3.9	70
40	1.33e-12	4.1	4.59e-13	5.7	7.52e-12	4.6	2.66e-12	5.8	1.42e-08	3.1	9.66e-09	3.9	70

5.4.3. Structural scheme

We have identified the two physical equations (31)-(32) or, alternatively, the upgrade version (31) and (33). At least two more equations are required to close the linear system.

- The 4thZD method consists in adding twice the structural equation HSE1(i) for variables Z_ρ, D_ρ and for variables Z_u, D_u, for all the inner nodes $i = 1, \cdots, I-1$. For the first node $i = 0$, the two missing equations are provided by the boundary conditions $Z_{\rho,0}$ and $u_{u,0}$ at $x = x_L$. We proceed in the same way for the other boundary $x = x_R$.
- The 6thZDS method requires the introduction of the second derivatives S_ρ and S_u and four additional equations. We use CSE1(i) and CSE2(i) for both ρ and u at the inner nodes $i = 1, \cdots, I-1$. At the boundary, we prescribe the two Dirichlet conditions, but two equations are still missing. We then complete the system with the CSE3(i) relations at node $i = 1$ and $i = I-1$ for the two variables.

Remark. Fix point method requires that the operator is a contraction. A usual trick to guarantee the convergence consists in, given the data at stage k, solving the linearized system to provide a candidate $\left(Z_\rho^{(k+1/2)}, Z_u^{(k+1/2)}, D_\rho^{(k+1/2)}, D_u^{(k+1/2)}\right)$. Then, we update the stage with a convex combination

$$Z_\rho^{(k+1)} = \theta Z_\rho^{(k+1/2)} + (1-\theta) Z_\rho^{(k)},$$

and the same for the other variables. We tune the coefficient θ to guarantee the convergence while avoiding too many iterations.

5.4.4. Benchmarks

The first numerical test concerns the subsonic case, where one considers the manufactured solution as follows,

$$\rho = x^2 + 0.5\cos(x) + 1, \quad u = 0.5x^2 + \sin(x) + 0.5, \quad p = \kappa \rho^\gamma,$$

with $\kappa = 1$ and $\gamma = 1.4$. Dirichlet boundary conditions are prescribed at both sides of the domain [0,1].

We report in Tables 9 the errors and convergence orders for the fourth-order 4thZD and sixth-order 6thZDS methods using the rough linearization together with the number of iterations. We use $\theta = 1/2$ to enforce the convergence of the procedure. Optimal order is achieved and no oscillations of the solution have been detected. The upgrade version of the linearization is provided in Table 10. The number of iterations is quite similar to the rough configuration, and the numerical

Table 11
Relative errors and convergence orders for the Isentropic Euler second Problem using 4thZD and 6thZDS using the rough linearization.

	4thZD								
I	error u	order	error ρ	order	error u'	order	error ρ'	order	its
20	1.31e-08	***	2.44e-09	***	1.80e-09	***	1.24e-08	***	69
40	8.64e-10	3.9	1.67e-10	3.9	1.21e-10	3.9	8.53e-10	3.9	69
80	5.56e-11	4.0	1.11e-11	3.9	7.72e-12	4.0	5.46e-11	4.0	68
160	3.59e-12	4.0	8.79e-13	3.7	4.71e-13	4.0	3.45e-12	4.0	67

	6thZDS												
I	error u	order	error ρ	order	error u'	order	error ρ'	order	error u''	order	error ρ''	order	its
10	1.02e-09	***	2.26e-09	***	1.38e-09	***	1.07e-08	***	4.63e-08	***	1.72e-06	***	69
20	2.13e-11	5.6	4.82e-11	5.6	2.90e-11	5.6	2.35e-10	5.5	3.52e-09	3.7	1.23e-07	3.8	68
30	1.83e-12	6.1	4.87e-12	5.7	2.80e-12	5.8	2.26e-11	5.8	8.58e-10	3.5	2.55e-08	3.9	69
40	2.82e-13	6.5	4.87e-12	5.0	5.19e-13	5.9	4.14e-12	5.9	4.26e-10	2.4	8.23e-09	3.9	69

Table 12
Relative errors and convergence orders for the Isentropic Euler second Problem using 4thZD and 6thZDS using the upgraded linearization.

	4thZD								
I	error u	order	error ρ	order	error u'	order	error ρ'	order	its
20	1.31e-08	***	2.44e-09	***	1.80e-09	***	1.24e-08	***	69
40	8.64e-10	3.9	1.67e-10	3.9	1.21e-10	3.9	8.53e-10	3.9	69
80	5.55e-11	4.0	1.11e-11	3.9	7.71e-12	4.0	5.46e-11	4.0	69
160	3.58e-12	4.0	8.79e-13	3.7	4.46e-13	4.1	3.45e-12	4.0	69

	6thZDS												
I	error u	order	error ρ	order	error u'	order	error ρ'	order	error u''	order	error ρ''	order	its
10	1.01e-09	***	2.26e-09	***	1.38e-09	***	1.07e-08	***	4.71e-08	***	1.72e-06	***	69
20	2.14e-11	5.6	4.80e-11	5.6	2.90e-11	5.6	2.35e-10	5.5	3.50e-09	3.75	1.23e-07	3.8	69
30	1.84e-12	6.0	4.88e-12	5.6	2.78e-12	5.8	2.26e-11	5.8	8.18e-10	3.6	2.55e-08	3.9	69
40	2.73e-13	6.6	1.14e-12	5.0	5.23e-13	5.8	4.12e-12	5.9	3.87e-10	2.6	8.21e-09	4.0	69

approximations are identical. In short, the new linearization does not substantially improve the convergence of the iterative method.

The second benchmark tackles the situation with a transition between subsonic and supersonic regimes. The manufactured solution is

$$\rho = x^2 + 0.5\cos(x) + 1, \quad u = 5x^2 + \sin(x) + 0.5 \quad p = k\rho^\gamma,$$

with $\kappa = 1$ and $\gamma = 1.4$. Dirichlet boundary conditions are prescribed at both ends of the domain [0,1].

Table 11 gives the errors and convergence orders for the fourth-order 4thZD and sixth-order 6thZDS methods using the rough linearization together with the number of iterations, while the upgrade version of the linearization is presented in Table 12. The number of iterations between the two algorithms is quite similar. Convergences are optimal, and no oscillation is detected.

5.5. Perfect gas euler system

The Euler system equipped with the perfect gas law is a more complex situation involving deeper entanglements between the density, velocity and pressure. Several compact schemes have been already proposed using the *a priori* WENO approach [58] or the *a posteriori* MOOD paradigm [32] to handle the discontinuities.

The non-conservative system reads

$$\begin{aligned} A(x) &= \rho\frac{du}{dx} + u\frac{d\rho}{dx}, \\ B(x) &= \rho u\frac{du}{dx} + \frac{dp}{dx}, \\ C(x) &= \rho^2 u\frac{d}{dx}\left(\frac{p}{\rho}\right) + (\gamma-1)\rho p\frac{du}{dx}. \end{aligned}$$

with ρ the density, u the velocity and p the pressure with $\gamma \in]1,3[$. Source terms $A(x)$, $B(x)$ and $C(x)$ are given functions together with the Dirichlet condition for ρ, u and p at the boundaries $x = x_L$ and x_R. We rewrite the equation in $Z-D$ variables

Table 13
Relative errors and convergence orders for the density using method 4thZD (left panel) and method 6thZDS (right panel).

	4thZD						
I	error ρ	ord	error ρ'	ord	its		
10	2.12e-07	***	1.38e-06	***	126		
20	9.39e-09	4.5	6.49e-08	4.4	124		
40	4.97e-10	4.2	3.54e-09	4.2	125		
60	9.32e-11	4.1	6.69e-10	4.1	126		
80	2.87e-11	4.1	6.69e-13	4.1	125		
	6thZDS						
I	error ρ	ord	error ρ'	ord	error ρ''	ord	its
10	1.09e-09	***	7.61e-09	***	2.13e-06	***	135
20	2.45e-11	5.5	2.01e-10	5.2	1.66e-07	3.7	140
30	2.45e-12	5.7	2.14e-11	5.5	3.55e-08	3.8	141
40	4.71e-13	5.7	4.24e-12	5.6	1.18e-08	3.8	142

Table 14
Relative errors and convergence orders for the velocity using method 4thZD (left panel) and method 6thZDS (right panel).

	4thZD						
I	error u	ord	error u'	ord	its		
10	5.21e-08	***	6.58e-09	***	126		
20	2.48e-09	4.4	3.19e-10	4.4	124		
40	1.37e-10	4.2	1.77e-11	4.2	125		
60	2.61e-11	4.1	3.35e-12	4.1	126		
80	8.08e-12	4.1	1.03-12	4.1	125		
	6thZDS						
I	error u	ord	error u'	ord	error u''	ord	its
10	7.22e-11	***	1.70e-10	***	1.15e-07	***	135
20	1.56e-12	5.5	5.51e-12	4.9	8.43e-09	3.8	140
30	1.61e-13	5.6	6.35e-13	5.3	1.80e-09	3.8	141
40	2.89e-14	6.0	1.22e-13	5.7	5.78e-09	4.0	142

Table 15
Relative errors and convergence orders for the pressure using method 4thZD (left panel) and method 6thZDS (right panel).

	4thZD						
I	error p	ord	error p'	ord	its		
10	2.85e-07	***	8.85e-07	***	126		
20	1.29e-08	4.5	4.46e-08	4.3	124		
40	6.91e-10	4.2	2.52e-09	4.1	125		
60	1.20e-10	4.1	4.82e-10	4.1	126		
80	4.01e-11	4.1	1.50-10	4.1	125		
	6thZDS						
I	error p	ord	error p'	ord	error p''	ord	its
10	3.69e-10	***	1.00e-09	***	8.54e-07	***	135
20	8.03e-12	5.5	2.92e-11	5.1	6.73e-08	3.7	140
30	7.92e-13	5.7	3.23e-12	5.4	1.44e-08	3.8	141
40	1.58e-13	5.6	6.04e-13	5.8	4.64e-09	3.9	142

$$A(x) = Z_\rho D_u + Z_u D_\rho,$$
$$B(x) = Z_\rho Z_u D_u + D_p,$$
$$C(x) = Z_\rho Z_u D_p - Z_p D_\rho + (\gamma - 1) Z_\rho Z_p D_u.$$

As in the isentropic case, we adopt a rough linearization of the system and, given the data at stage k, we compute the new stage with

$$A(x) = Z_\rho^{(k+1)} D_u^{(k)} + Z_u^{(k)} D_\rho^{(k+1)},$$
$$B(x) = Z_\rho^{(k)} Z_u^{(k)} D_u^{(k+1)} + D_p^{(k+1)},$$

$$C(x) = Z_\rho^{(k)} Z_u^{(k)} D_p^{(k+1)} - Z_p^{(k+1)} D_\rho^{(k)} + (\gamma - 1) Z_\rho^{(k)} Z_p^{(k+1)} D_u^{(k)}.$$

The numerical test concerns a smooth transition from supersonic to subsonic regime with the following manufactured solution

$$\rho = x^2 + 0.5\cos(x) + 1, \qquad u = 0.5x^2 + \sin(x) + 0.5; \qquad p = 2 - \frac{x^3}{3} - \frac{\sin(x)}{2}.$$

Right-hand side source term A, B and C are computed while Dirichlet boundary conditions are prescribed at both ends of the domain [0,1].

Tables 13, 14, and 15 provide the errors and convergence orders for the density, velocity and pressure respectively. The left table corresponds to the fourth-order `4thZD` method, while the right table reports the information for the sixth-order `6thZDS` method. Similarly to the other benchmarks, we obtain the optimal fourth-order of accuracy for the first scheme both for the function and the derivative. The sixth-order is achieved by the function and its first derivative, but the second derivative accuracy is stuck to the fourth-order. No convergence problem has been reported and the number of iterations is almost the same independently of the grid size.

6. Conclusion

We have proposed a new paradigm for elaborating compact schemes to provide accurate approximations of smooth solutions. The method involves the function and its derivatives approximations at the grid nodes, and relies on the construction of structural equations deriving from the kernels of a matrix that gathers the variables belonging to a small stencil. Numerical schemes are then elaborated from the combinations of physical equations and structural relations to equal the number of unknowns. We have analysed the spectral resolution of the most common structural equations and performed numerical tests to address both the stability and accuracy issues for popular linear and non-linear problems. The two- and three-dimensional cases have not been tackled, since we aim at focusing on the proof of concept and detailing the construction for the one-dimensional problem. The higher dimension will be considered by dimensional splitting together with an ADI procedure that enables to rewrite the d-dimensional problem into a series of one-dimensional problems.

Data availability

No data was used for the research described in the article.

Acknowledgements

S. Clain acknowledges the financial support by Portuguese Funds through Foundation for Science and Technology (FCT) in the framework of the Strategic Funding UIDB/00324/2020.

R. M. S. Pereira acknowledges the financial support by Portuguese Funds through Foundation for Science and Technology (FCT) in the framework of the Strategic Funding UIDB/04650/2020.

P. A. Pereira acknowledges the financial support by Portuguese Funds through Foundation for Science and Technology (FCT) in the framework of the Strategic Funding UIDB/00013/2020.

Diogo Lopes acknowledges the financial support by national funds (PIDDAC), through the FCT – Fundação para a Ciência e a Tecnologia and FCT/MCTES under the scope of the projects UIDB/05549/2020 and UIDP/05549/2020.

S. Clain and R. M.Pereira acknowledge the financial support by FEDER – Fundo Europeu de Desenvolvimento Regional, through COMPETE 2020 – Programa Operacional Fatores de Competitividade, and the National Funds through FCT, project N°. POCI-01-0145-FEDER-028118.

Appendix A. Historical notes

Compact finite difference method dates back to the early sixties with the publication of the Collatz's book in 1960 [11] and his *Mehrstellenverfahren* formula. Quoting Osborne in the paper of 1967 [41], the objective is " *to provide general schemes for generating difference approximations which make the best use of available information in the sense of minimizing truncation error*". Different technologies have proposed all along of six decades, and we roughly distinguish two different approaches for elaborating compact schemes: the methods that involve the operators/equations such as the *Operator Compact Implicit* (OCI) method; the methods that only involve relations between the approximations and the derivatives, independently of the underlying problem, like the *High Order Compact* (HOC) method.

To better highlight the differences, let us consider the simple linear steady-state problem

$$L(\phi) \equiv a(x)\phi''(x) + b(x)\phi'(x) + c(x)\phi(x) = f(x), \tag{A.1}$$

with appropriate boundary conditions while denoting ϕ_i the approximation of $\phi(x_i)$ over a grid $x_i = i\Delta x$, $i = 0, 1, \ldots, I$.

- The *Operator Compact Implicit* (OCI) method [10], also named *Elimination method* in the review of [14] p. 52, consists in coupling a classical finite difference scheme (the left-hand side of (A.2)) with linear combination of the operator (the

right-hand side of (A.2))

$$\sum_{\ell=-r}^{r} \alpha_{i,\ell}\phi_{i+\ell} = \sum_{\ell=-r}^{r} \beta_{i,\ell} L(\phi)_{i+\ell} \tag{A.2}$$

The coefficients are determined in order to be consistent with the highest degree as possible polynomials while exactly satisfying equation (A.1). The Numerov scheme [39] is a popular example of OCI scheme for linear diffusion reaction equation. We highlight two important points: (i) the method is problem-dependent in the sense that coefficients α and β depend on the equation; (ii) it only deals with approximations ϕ_i and does not introduce the derivative approximations. It may result in a discrepancy of the accuracy for the first or second derivatives, and the large stencil of the neighbour nodes leads to a high condition number of the whole linear system.

The *High-Order Difference approximation with Identity Expansion* (HODIE) formulation [33] is an extension of the original OCI method by adding new degrees of freedom to the original finite difference method, introducing new parameters β to the right-hand side approximation:

$$\sum_{\ell=-r}^{r} \alpha_{i+\ell}\phi_{i+\ell} = \sum_{\ell=-L}^{L} \beta_{i,\ell} f_{i,\ell}$$

where $f_{i,\ell} = f(\xi_{i,\ell})$ are evaluated on a sub-grid $\xi_{i,\ell}$ on interval $[x_{i-r}, x_{i+r}]$.

- The *High Order Compact* (HOC) method, also called *Hermitian* method [55], and also labelled as *implicit method* in [14] p. 40 is based on approximations Z_i, D_i and S_i of the function $\phi(x_i)$ and its derivatives $\phi'(x_i)$, $\phi''(x_i)$ respectively, with $i = 0, \cdots, I$. On the one hand, the approximations are substituted in equation (A.1) and provide the physical discrete equation

$$a(x_i)S_i + b(x_i)D_i + c(x_i)Z_i = f(x_i). \tag{A.3}$$

On the other hand, relations between the unknowns S, D and Z over a compact stencil are expressed in the form

$$\sum_{\ell=-s}^{r} \alpha_{i+\ell}Z_{i+\ell} + \sum_{\ell=-s}^{r} \beta_{i+\ell}D_{i+\ell} = 0, \tag{A.4}$$

$$\sum_{\ell=-s}^{r} \alpha'_{i+\ell}Z_{i+\ell} + \sum_{\ell=-s}^{r} \gamma_{i+\ell}S_{i+\ell} = 0. \tag{A.5}$$

Coefficients α, β and α', γ of (A.4) and (A.5) are determined to provide accuracy and stability. The Hermitian scheme proposed in [55] is a very popular example of HOC method. We highlight two important aspects of the method: (i) coefficients α, β and α', γ are independent of the problem and only rely on the grid structure; (ii) first and second order derivatives are also the unknowns of the problem; (iii) combining equations (A.4) and (A.5) together with the discrete physical equation (A.3) provides a large $3(I+1)$ system in Z, D, S to solve.

The origin of the OCI method [40] is derived from the construction of a local four-degree polynomial approximation of the solution and its second derivative over a three-point stencil to provide fourth-order approximations. The method is generalized in [41] for a large class of operators. From those pioneer papers, several authors have formalized the OCI scheme [10,51]. Doedel presents an extension of the OCI method where the collocation points of the solution and the operator approximations (the right-hand side source term) are different [12], equation (2.5), providing more degrees of freedom and increasing the accuracy (see also [34]). The author also introduces compact schemes for the boundary conditions to preserve the optimal accuracy. Applications to the wave equation are presented in [34] while non-linear systems such as the shallow water equations are solved with an OCI method in [38]. A more advanced HODIE formulation is proposed in [2,33,50] and achieves a very-high order of accuracy. Nevertheless, it turns to be more computational expensive for non-linear problems since all the coefficients have to be recomputed in the iterative linearization procedure.

We can trace back the first HOC method to the visionary paper of Bickley [3] in 1968. A short paper but with the main idea about the Hermitian compact scheme construction, considering Z and D as unknowns. In his conclusion, the author highlights that *"these simple experiments prove that the method is potentially useful"*. Following this pioneer work, Albasiny and Hoskins [1] produced in the same year a generalization of the Bickley method over a uniform grid. In particular, the implicit relation between Z and S is given in the paper. At last, the article of Fyfe [17] in 1969 gives the readable version of the HOC method. The discrete physical equation is explicitly mentioned (equation (21) in the paper) together with the relations between Z, D and S (equations (5)-(6) of the document). Moreover, the author proves an error estimate that concludes the method is of order four.

The modern HOC (hermitian) finite difference method has been published in three independent papers in 1975: (i) Y. Adam [55] for the parabolic equation; (ii) S. G. Rubin and R. A. Graves [45] for viscous flow; (iii) R. Hirsh [25] using the Padé approximations. Curiously, the authors reached to similar results using very different approaches. Adam establishes the relation between Z, D and S by setting, *a priori*, the linear combinations between function and derivatives. Then he determines the coefficients by achieving the highest order of consistency. Rubin and Graves, following [17], use cubic spline

for approximating the solution and deduce relations between Z, D and Z, S. In both papers, Z, D and S are unknowns leading to a larger linear system to solve. Regarded to the equivalence of the different approaches (spline, hermitian, Padé method), we quote a note in the introduction of [44] *"The authors have examined these procedures [...] and found them to be, in fact, identical"*.

The next decade brought consolidation and extensions of the compact finite difference theory and several issues were tackled such as the boundary condition [2,50], the stability [33], upwind scheme [6,27], non-equidistant mesh [22] and non-linear fluid mechanics problems. The Ph.D. thesis of Pettigrew [14] provides an excellent review of the state of the art at the end of the eighties. Spectral resolution ability turns to be one of the major issues in the nineties. The pioneer work of Lele in 1992 [29] proposes a general construction of the compact schemes and a spectral analysis. As mentioned in [54], the number of Points Per Wavelength (PPW) limits the smallest scale of resolution and *"implicit compact schemes had better resolution than regular explicit schemes of the same order of accuracy and computational stencil"*. The design of both accurate and high-resolution schemes has then been tackled by several authors [18,26,36,42] during the decade.

Regarded to the Combined Compact Scheme (CCS) of Chu and Fan [7] published in 1998, it is noteworthy to see that, in the study of Rubin and Khosla in 1976 [43], p. 10, the authors had already proposed the sixth-order three-point compact method using a fifth-order spline reconstruction, very similar to the Combined Compact Scheme. The technical document has been forgotten by the community, while it contains a very interesting review of the HOC method developed at that time. Moreover, fourth- and sixth-order simulations of non-trivial applications in one-dimension and two-dimensional geometries represent an incredible technical feature in the middle of the seventies.

We also mention the so-called Super Compact Finite Difference (SCFD) scheme introduced by Fu and Ma [16,35] of arbitrary order with minimal stencil size, where the authors use 3-points higher $2M-1$ derivatives but with a specific odd-even pattern for the combinations (see also [20,21]). Nevertheless, on the one hand, they do not take advantage of all the intermediate derivatives as it is done in the CCD method and, on the other hand, the method requires that the solution is very smooth with no steep variations (boundary layer problem for instance). Indeed, the SCFD uses fourth- or fifth-order derivatives when the CCD only handles first and second order derivatives.

References

[1] E.L. Albasiny, W.D. Hoskins, Cubic spline solutions to two-point boundary value problems, Comput. J. 11 (1968) 151–153.
[2] A.E. Berger, J.M. Solomon, M. Ciment, S.H. Leventhal, B.C. Weinberg, Generalized OCI schemes for boundary layer problems, Math. Comput. 35 (11) (1980) 695–731.
[3] W.G. Bickley, Piecewise cubic interpolation and two-point boundary problem, Comput. J. 11 (1968) 206–208.
[4] B.J. Boersma, A 6th order staggered compact finite difference method for the incompressible navier–Stokes and scalar transport equations, J. Comput. Phys. 230 (2011) 4940–4954.
[5] P. Chiu, T.W. Sheu, On the development of a dispersion-relation-preserving dual-compact upwind scheme for convection–diffusion equation, J. Comput. Phys. 228 (2009) 3640–3655.
[6] I. Christie, Upwind compact finite difference scheme, J. Comput. Phys. 59 (1985) 353–368.
[7] P. Chu, C. Fan, A three-point combined compact difference scheme, J. Comput. Phys. 140 (1998) 370–399.
[8] P. Chu, C. Fan, A three-point sixth-order nonuniform combined compact difference scheme, J. Comput. Phys. 148 (1999) 663–674.
[9] P. Chu, C. Fan, A three-point sixth-order staggered combined compact difference scheme, Math Comput Model 32 (2000) 323–340.
[10] M. Ciment, S.H. Leventhal, B.C. Weinberg, The operator compact implicit method for parabolic equations, J.Comp.Phys. 28 (1978) 135–166.
[11] L. Collatz, The Numerical Treatment of Differential Equations, 3rd ed., Springer-Verlag, Berlin., 1960.
[12] E.J. Doedel, The construction of finite difference approximations to ordinary differential equations, SIAM J. Numer. Anal. 15 (3) (1978) 450–465.
[13] B. Engquist, A. Majda, Radiation boundary conditions for acoustic and elastic wave calculations, Commun. Pure Appl. Math. 32 (1979) 313–357.
[14] M.F. Pettigrew, On Compact Finite Difference Schemes With Applications to Moving Boundary Problems, Ph.D. thesis, Western University, 1989.
[15] P. Frolkovič, M. Žeravý, High resolution compact implicit numerical scheme for conservation laws, Appl. Math. Comput. 442 (2023) 127720.
[16] D. Fu, Y. Ma, High resolution schemes, Computational Fluid Dynamic Review. M. Hafez and K. Oshima, Eds., Johnn Wiley and Sons, 1995.
[17] D.J. Fyfe, The use of cubic splines in the solution of two-point boundary value problems, Comput. J. 12 (1969) 188–192.
[18] L. Gamet, F. Ducros, F. Nicoud, T. Poinsot, Compact finite difference schemes on non-uniform meshes. application to direct numerical simulations of compressible flows, Int. J. Numer. Methods Fluids 29 (1999) 159–191.
[19] L. Ge, J. Zhang, High accuracy solution of convection diffusion equation with boundary layers on nonuniform grids, J. Comput. Phys. 171 (2001) 560.
[20] S. Ghader, A.R.M.V. Esfahanian, On the spectral convergence of the super compact finite-difference schemes for the f-plane shallow-water equations, Mon. Weather Rev. 137 (7) (2009) 2393–2406.
[21] S. Ghadera, J. Nordström, High-order compact finite difference schemes for the spherical shallow water equations, Int. J. Numer. Meth. Fluids (2013) 1–27.
[22] W.I. Goedheer, J.H.H.M. Potters, A compact finite difference scheme on a non-equidistant mesh, J. Comput. Phys. 61 (1985) 269–279.
[23] Y. Guo, Y. f. Shi, Y. m. Li, A fifth-order finite volume weighted compact scheme for solving one-dimensional burger's equation, Appl. Math. Comput. 281 (2016) 172–185.
[24] G. Gürarslan, Numerical modelling of linear and nonlinear diffusion equations by compact finite difference method, Appl. Math. Comput. 216 (2010) 2472–2478.
[25] R. Hirsh, Higher order accurate difference solution of fluid mechanics problems by a compact differencing technique, Computat. Phys. 19 (1975) 90–109.
[26] J.W. Kim, D.T. Lee, Optimized compact finite difference schemes with maximum resolution, AIAA J. 34 (5) (1996) 887–893.
[27] H.-O. Kreiss, T.A. Manteuffel, Supra-convergent schemes on irregular grids, Math. Comput. 47 (176) (1986) 537–554.
[28] S. Laizet, E. Lamballais, High-order compact schemes for incompressible flows: a simple and efficient method with quasi-spectral accuracy, J. Comput. Phys. 228 (2009) 5989–6015.
[29] S.K. Lele, Compact finite difference schemes with spectral-like resolution, J. Comput. Phys. 103 (1992) 16–42.
[30] W. Liao, An implicit fourth-order compact finite difference scheme for one-dimensional burger's equation, Appl. Math. Comput. 206 (2008) 755–764.
[31] X. Liu, S. Zhang, H. Zhang, C.-W. Shu, A new class of central compact schemes with spectral-like resolution i: linear schemes, J. Comput. Phys. 248 (2013) 235–256.
[32] R. Loubère, R. Turpault, A. Bourriaud, A MOOD-like compact high order finite volume scheme with adaptive mesh refinement, Appl. Math. Comput. 443 (2023) 127792.
[33] R.E. Lynch, J.R. Rice, A high-order difference method for differential equations, Math. Comput. 14 (150) (1980) 333–372.

[34] S.H.L. M. Ciment, A note on the operator compact implicit method for the wave equation, Math. Comp. 22 (141) (1978) 143–147.
[35] Y. Ma, D. Fu, Super compact finite difference method (SCFDM) with arbitrary high accuracy, Comput. Fluid Dyn. J. 5 (1996) 259–276.
[36] K. Mahesh, A family of high order finite difference schemes with good spectral resolution, J. Comput. Phys. 145 (1998) 332–358.
[37] S. Nagarajan, S.K. Lele, J.H. Ferziger, A robust high-order compact method for large eddy simulation, J Comput. Phys. 191 (2003) 392–419.
[38] I.M. Navon, H.A. Riphagen, An implicit compact fourth-order algorithm for solving the shhallow-Water equations in conservative-law form, Mon. Weather Rev. 107 (9) (1979) 1107–1127.
[39] B.V. Numerov, A method of extrapolation of perturbations, Roy. Ast. Soc. Monthly Notices 84 (1927) 592–601.
[40] M.R. Osborne, A method for finite-difference approximation to ordinary differential equations, Comput. J. 7 (1964) 58–65.
[41] M.R. Osborne, Minimizing truncation error in finite difference approximations to ordinary differential equations, Math. Comp. 21 (1967) 133–145.
[42] M.F. Pettigrew, H. Rasmussen, A compact method for second-order boundary values problems on non-uniform grids, Comput. Math. Applic. 31 (9) (1996) 1–16.
[43] S.G. Rubin, P.K. Khosla, Higher order numerical methods derived from three-point polynomial interpolation, NASA Technical paper CR-2735 (1976) 1–73.
[44] S.G. Rubin, P.K. Khosla, Numerical method based on polynomial spline interpolation, Proceeding of the fifth international conference on numerical methods in fluid dynamics, Lecture notes in physics, Springer-Verlag 59 (1976) 370–377.
[45] R.A. Graves, S.G. Rubin, Viscous flow solutions with a cubic spline approximation, Comput. Fluids 3 (1975) 1–36.
[46] A.S. Sabau, P.E. Raad, Comparisons of compact and classical finite difference solutions of stiff problems on nonuniform grids, Comput. Fluids 28 (1999) 361–384.
[47] M. Sari, G. Gürarslan, A sixth-order compact finite difference scheme to the numerical solutions of burger's equation, Appl. Math. Comput. 208 (2009) 475–483.
[48] A. Shah, L. Yuan, A. Khan, Upwind compact finite difference scheme for time-accurate solution of the incompressible navier–Stokes equations, Appl. Math. Comput. 215 (2010) 3201–3213.
[49] R.K. Shukla, X. Zhong, Derivation of high-order compact finite difference schemes for non-uniform grid using polynomial interpolation, J. Comput. Phys. 204 (2005) 404–429.
[50] B. Swartz, Compact implicit difference schemes for a differential equation's side condition, Math. Comput. 35 (151) (1980) 733–746.
[51] B.K. Swartz, The construction of finite difference analog of some finite element chemes, Mathematical aspects of finite Elements in partial differential equations (C. de Boor Ed.) Academic Press (1974) 279–312.
[52] J. Wang, W. Zhong, J. Zhang, A general meshsize fourth-order compact difference discretization scheme for 3d poisson equation, Appl. Math. Comput. 183 (2006) 804–812.
[53] Z. Wang, Y. Ge, H.-W. Sun, T. Sun, Sixth-order quasi-compact difference schemes for 2d and 3d helmholtz equations, Appl. Math. Comput. 431 (2022) 127347.
[54] R. Wilson, A. Demuren, M. Carpenter, Higher-order compact schemes for numerical simulation of incompressible flows, ASA/CR, ICASE Report 98-13 (1998) 1–42.
[55] Y. Adam, A hermitian finite difference method for the solution of parabolic equations, Comput. Maths. with Appls. 1 (1975) 396–406.
[56] X. Yang, Y. Ge, L. Zhang, A class of high-order compact difference schemes for solving the burger's equations, Appl. Math. Comput. 358 (2019) 394–417.
[57] M.U. Zapata, R.I. Balam, High-order implicit finite difference schemes for the two-dimensional poisson equation, Appl. Math. Comput. 309 (2017) 222–244.
[58] H. Zhang, F. Zhang, C. Xu, Towards optimal high-order compact schemes for simulating compressible flows, Appl. Math. Comput. 355 (2019) 221–237.
[59] X. Zhong, M. Tatineni, High-order non-uniform grid schemes for numerical simulation of hypersonic boundary-layer stability and transition, J. Comput. Phys. 190 (2003) 419.